TEXAS
The University of Texas at Austin

Projecting Need for a COVID-19 Alternative Care Site (ACS) Austin, TX

Haoxiang Yang, Michael Lachmann, Özge Sürer, Spencer J. Fox, David P. Morton, Lauren Ancel Meyers

The University of Texas at Austin
COVID-19 Modeling Consortium

utpandemics@austin.utexas.edu

Projecting Need for a COVID-19 Alternate Care Site (ACS), Austin, TX

January 8, 2021

[The University of Texas COVID-19 Modeling Consortium]
Contributors: Haoxiang Yang, Michael Lachmann, Özge Sürer, Spencer J. Fox, David P. Morton, Lauren Ancel Meyers
Contact: utpandemics@austin.utexas.edu

Overview

To support the city of Austin and Travis County in responding to the threatening rise in COVID-19 hospitalizations, we used a data-driven model of COVID-19 transmission in the Austin-Round Rock MSA to project hospitalizations until February 4th, estimate the risk that cases will exceeding local capacity, and determine effective triggers for opening an alternative care site (ACS) to expand capacity. Note that the results presented herein are based on multiple assumptions about the transmission rate and age-specific severity of COVID-19 and do not represent the full range of uncertainty. Rather, they are meant to provide plausible scenarios for COVID-19 healthcare demand and inform decisions that balance the high costs of establishing an ACS with the risks of outstripping local healthcare capacity.

Based on information provided by the city of Austin, we assume that an ACS can be ready to accept patients two weeks after it is triggered. Our projections indicate the following:

- There is a 21% chance that COVID-19 cases requiring hospital care will exceed estimated capacity within two weeks (by Jan 22) and a 40% chance this will occur within three weeks (by Jan 29).
- The ACS launch should be triggered when the **seven-day rolling average of COVID-19 hospital admissions exceeds 70** to provide a 95% guarantee that Austin will maintain sufficient hospital capacity while minimizing the risk of a false alarm (unnecessary launch of the ACS).
- Initiating the ACS when hospitals reach 85% of their estimated COVID-19 capacity (rather than at the recommended trigger) would lead to a 40% chance of exceeding capacity before the ACS is available.

We are posting these results prior to peer review to provide intuition for both policy makers and the public regarding the immediate threat of COVID-19 to our healthcare systems.

Austin COVID-19 models

The appendices below describe the methods in detail. We use mathematical equations to track the changing numbers of individuals who are susceptible (not yet infected), infected, hospitalized, recovered, and deceased. Our forecasting model uses iterated filtering [1] to estimate daily transmission rates in Austin from a combination of local hospital data (COVID-19 admissions, discharges and deaths) as well as SafeGraph mobility trends (cell phone-based estimates of hours spent at home and daily trips to public points-of-interest such as grocery stores, restaurants, bars and parks [2]). We use the estimated transmission rates to project COVID-19 cases, hospitalizations, ICU visits and deaths several weeks ahead. Our ACS trigger analysis uses a method [3] originally developed to derive the COVID-19 hospital admissions thresholds displayed on Austin's Key Indicators for Staging Dashboard [4].

Our projections assume the following:

- Epidemic seeding: February 17th, 2020 with 1 infected adult
- Transmission rates are modulated by age-specific contact patterns
- Following infection, cases go through multiple stages of infection:

  Stage 1: Pre-symptomatic and non-contagious for an average of 2.9 days

  Stage 2: Pre-symptomatic contagious for an average of 2.3 days (44% of transmission events occur during this period)

  Stage 3: Symptomatic contagious or asymptomatic contagious for an average of 4 days. The model assumes that 43% of all infections are asymptomatic and that asymptomatic cases are 67% as infectious as symptomatic cases.
- COVID-19 hospitalization and mortality rates depend on age and risk group:
  - The overall infection hospitalization rate (IHR) is 4.2%
  - The overall infection fatality rate (IFR) is 0.54%
- Austin Area COVID-19 hospital and ICU capacity: 1500 and 200 patients
- Set-up time for Alternative Care Site (ACS): 14 days

COVID-19 Hospital and ICU Projections

Based on COVID-19 hospitalization data through January 7th, we estimate that the reproduction number in Austin is likely above one with a 94% chance the epidemic will continue to grow. Specifically, R_t = 1.27 [95%CI: 0.93 - 2.07].

Figure 1 projects COVID-19 hospitalizations and ICU patients in the Austin Area through February 4th. The *spaghetti line* projections in each figure capture our uncertainty regarding the current transmission rate virus. While most trend upwards a few are relatively flat. Each line represents an equally likely future path and the bold trend line is the median across all projections. The horizontal lines in each graph indicate the estimated COVID-19 healthcare capacity for the Austin Area. The Austin Executive COVID-19 Task Force has estimated that across all hospitals in the five-county metropolitan area, the maximum COVID-19 hospital surge capacity is 1,500 patients and the maximum COVID-19 ICU surge capacity is about 200 patients. Recent COVID-19 hospitalization data suggest that between 30% and 40% of hospitalized COVID-19 patients are in ICUs. The Austin COVID-19 Healthcare Dashboard provides daily estimates of the local reproduction number and four-week healthcare projections.

Assuming that policies and behavior do not change, our model projects the following for two weeks ahead (January 22nd):

- Daily COVID-19 hospital census will reach 920 [95% CrI: 600-1900] patients
- 20% chance of exceeding 1,500 COVID-19 hospitalizations by January 22nd
- Daily COVID-19 ICU census will reach 260 [95% CrI: 170-540] patients
- 90% chance of exceeding 200 COVID-19 ICU patients by January 22nd

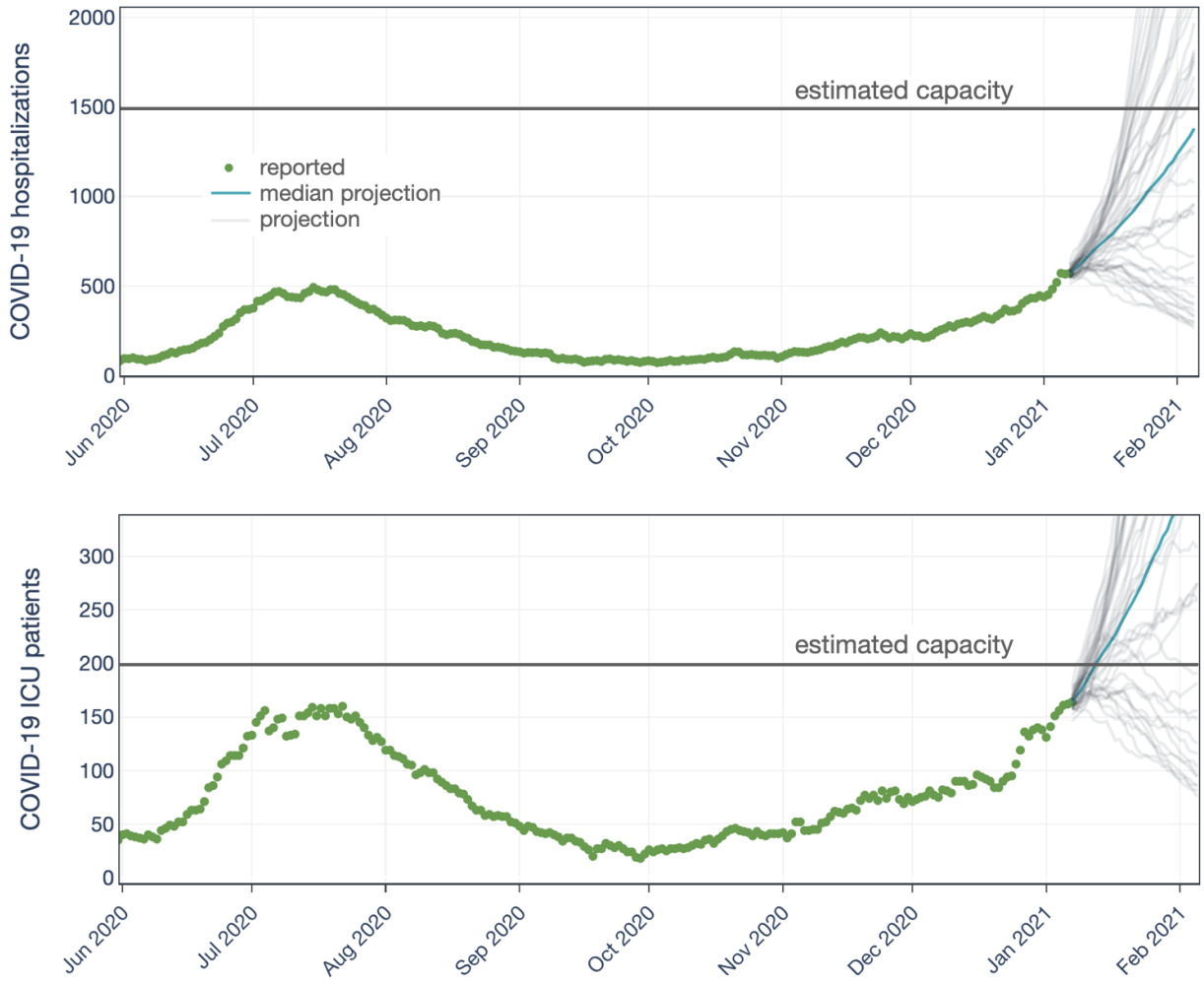

Figure 1: Projected COVID-19 hospital (top) and ICU (bottom) census in the Austin-Round Rock MSA through February 4, 2021. Green points represent the reported daily census. Grey "spaghetti" lines represent equally likely projections and the blue line indicates the median trend based on the range of transmission rates estimated as of January 7, 2021. Differences between lines are caused by uncertainty in the model inputs as well as variation in individual behavior and disease progression.

Alternative Care Site (ACS) Analysis

Figure 2 projects COVID-19 hospitalizations under two different scenarios for launching an ACS. The top graph assumes that a 550 bed ACS is opened when the rolling seven-day average of hospital admissions surpasses 70. The bottom graph assumes that Austin waits until COVID-19 hospital patients exceed at least 85% of local capacity (1,270 of 1,500 available beds).

Our analyses assume that local COVID-19 hospital capacity is 1,500 patients, it takes two weeks to launch the ACS, and the ACS will remain open for 100 days. We use our model to identify an optimal trigger for launching the ACS that simultaneously ensures sufficient capacity and avoids false alarms leading to wasted resources. Our analyses suggest the following:

- Recommended ACS threshold: Seven-day average of **70 COVID-19 hospital admissions**
- Recommended ACS capacity: **550 patients**
- Chance of a shortfall if trigger is delayed until hospitals reach 85% of their COVID-19 capacity: **40%**

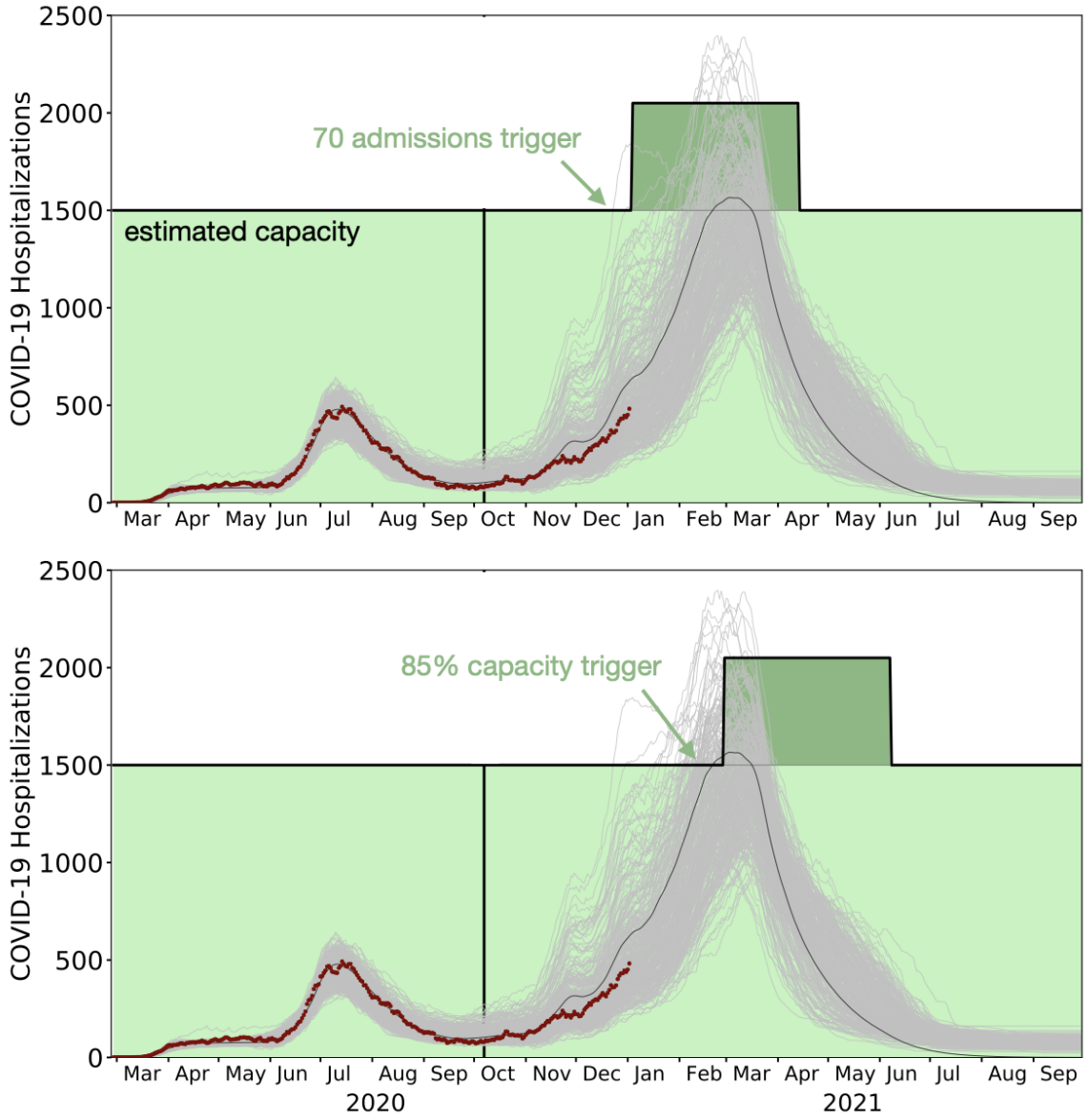

Figure 2: Projected timing of alternative care site (ACS) to expand capacity during COVID-19 hospital surges in the Austin-Round Rock MSA. Light green shading indicates estimated hospital capacity and dark green shading indicates additional ACS capacity. We assume that 550 additional beds become available two weeks after the ACS is triggered and that the ACS remains open for 100 days. The top graph assumes that the ACS is triggered when the rolling seven-day average of COVID-19 hospital admissions reaches the optimized threshold of 70. The bottom graph assumes that the ACS is triggered when COVID-19 hospitalizations reach 85% of total capacity (1,270 of 1,500 available beds). The red points are reported hospitalizations, the vertical black line indicates the beginning of the projection period, the grey “spaghetti” lines are equally likely stochastic projections, the light black curve is the deterministic projection.Differences between lines are caused by uncertainty in the model inputs as well as variation in individual behavior and disease progression.

References

1. Ionides EL, Nguyen D, Atchadé Y, Stoev S, King AA. Inference for dynamic and latent variable models via iterated, perturbed Bayes maps. Proc Natl Acad Sci U S A. 2015;112: 719–724.

2. Gao S, Rao J, Kang Y, Liang Y, Kruse J. Mapping county-level mobility pattern changes in the United States in response to COVID-19. arXiv [physics.soc-ph]. 2020. Available: http://arxiv.org/abs/2004.04544

3. Duque D, Morton DP, Singh B, Du Z, Pasco R, Meyers LA. Timing social distancing to avert unmanageable COVID-19 hospital surges. Proceedings of the National Academy of Sciences. 2020. Available: https://www.pnas.org/content/early/2020/07/28/2009033117.short

4. ArcGIS Dashboards. [cited 7 Jan 2021]. Available: https://austin.maps.arcgis.com/apps/opsdashboard/index.html#/0ad7fa50ba504e73be9945ec2a7841cb

Appendix 1: Projecting COVID-19 Healthcare Demand

COVID-19 Epidemic Model Structure and Parameters

The model structure is diagrammed in Figure A1 and described in the equations below.
For each age and risk group, we build a separate set of compartments to model the transitions between the states: susceptible (S), exposed (E), pre-symptomatic infectious (P^Y), pre-asymptomatic infectious (P^A), symptomatic infectious (I^Y), asymptomatic infectious (I^A), symptomatic infectious that are hospitalized (I^H), recovered (R), and deceased (D). The symbols S, E, P^Y, P^A ,I^Y, I^A, I^H, R, and D denote the number of people in that state in the given age/risk group and the total size of the age/risk group is

$$N = S + E + P^Y + P^A + I^Y + I^A + I^H + R + D.$$

The deterministic model for individuals in age group a and risk group r is given by:

$$\frac{dS_{a,r}}{dt} = -S_{a,r} \cdot \sum_{i \in A} \sum_{j \in K} (I^Y_{i,j}\omega^Y + I^A_{i,j}\omega^A + P^Y_{i,j}\omega^{PY} + P^A_{i,j}\omega^{PA})\beta(t)\phi_{a,i}/N_i$$

$$\frac{dE_{a,r}}{dt} = S_{a,r} \cdot \sum_{i \in A} \sum_{j \in K} (I^Y_{i,j}\omega^Y + I^A_{i,j}\omega^A + P^Y_{i,j}\omega^{PY} + P^A_{i,j}\omega^{PA})\beta(t)\phi_{a,i}/N_i - \sigma E_{a,r}$$

$$\frac{dP^A_{a,r}}{dt} = (1-\tau)\sigma E_{a,r} - \rho^A P^A_{a,r}$$

$$\frac{dP^Y_{a,r}}{dt} = \tau\sigma E_{a,r} - \rho^Y P^Y_{a,r}$$

$$\frac{dI^A_{a,r}}{dt} = \rho^A P^A_{a,r} - \gamma^A I^A_{a,r}$$

$$\frac{dI^Y_{a,r}}{dt} = \rho^Y P^Y_{a,r} - (1-\pi)\gamma^Y I^Y_{a,r} - \pi\eta I^Y_{a,r}$$

$$\frac{dI^H_{a,r}}{dt} = \pi\eta I^Y_{a,r} - (1-\nu)\gamma^H(t) I^H_{a,r} - \nu\mu(t) I^H_{a,r}$$

$$\frac{dR_{a,r}}{dt} = \gamma^A I^A_{a,r} + (1-\pi)\gamma^Y I^Y_{a,r} + (1-\nu)\gamma^H(t) I^H_{a,r}$$

$$\frac{dD_{a,r}}{dt} = \nu\mu(t) I^H_{a,r}$$

where A and K are all possible age and risk groups, ^{A} , ^{Y}, ^{PA}, ω^{PY} are the relative infectiousness of the I^A, I^Y, I^{PA}, I^{PY} compartments, respectively, β is transmission rate, $_{a,i}$ is the mixing rate between age group a, $i \in A$, and γ^A, γ^Y, $\gamma^H(t)$ are the recovery rates for the

I^A, I^Y, I^H compartments, respectively, σ is the exposed rate, ρ^A, ρ^Y are the pre-(a)symptomatic rates, τ is the symptomatic ratio, π is the proportion of symptomatic individuals requiring hospitalization, η is rate at which hospitalized cases enter the hospital following symptom onset, ν is mortality rate for hospitalized cases, and $\mu(t)$ is daily instantaneous rate at which terminal patients die.

We simulate the model using a stochastic implementation of the deterministic equations. Transitions between compartments are governed using the τ-leap method [1,2] with key parameters given in Table A1-2. We simulate the model according to the following equations:

$$S_{a,r}(t+1) - S_{a,r}(t) = -P_1$$
$$E_{a,r}(t+1) - E_{a,r}(t) = P_1 - P_2$$
$$P^A_{a,r}(t+1) - P^A_{a,r}(t) = (1-\tau)P_2 - P_3$$
$$P^Y_{a,r}(t+1) - P^Y_{a,r}(t) = \tau P_2 - P_4$$
$$I^A_{a,r}(t+1) - I^A_{a,r}(t) = P_3 - P_5$$
$$I^Y_{a,r}(t+1) - I^Y_{a,r}(t) = P_4 - P_6 - P_7$$
$$I^H_{a,r}(t+1) - I^H_{a,r}(t) = P_7 - P_8 - P_9$$
$$R_{a,r}(t+1) - R_{a,r}(t) = P_5 + P_6 + P_8$$

with

$$P_1 \sim B(n = S_{a,r}(t),\, p = 1 - e^{-(F_{a,r}(t))\cdot dt})$$
$$P_2 \sim B(n = E_{a,r}(t),\, p = 1 - e^{-(\sigma)\cdot dt})$$
$$P_3 \sim B(n = P^A_{a,r}(t),\, p = 1 - e^{-(\rho^A)\cdot dt})$$
$$P_4 \sim B(n = P^Y_{a,r}(t),\, p = 1 - e^{-(\rho^Y)\cdot dt})$$
$$P_5 \sim B(n = I^A_{a,r}(t),\, p = 1 - e^{-(\gamma^A)\cdot dt})$$
$$P_6 \sim B(n = I^Y_{a,r}(t),\, p = 1 - e^{-((1-\pi)\gamma^Y)\cdot dt})$$
$$P_7 \sim B(n = I^Y_{a,r}(t),\, p = 1 - e^{-(\pi\eta)\cdot dt})$$
$$P_8 \sim B(n = I^H_a,\, p = 1 - e^{-((1-\nu)\gamma^H(t))\cdot dt})$$
$$P_9 \sim B(n = I^H_{a,r}(t),\, p = 1 - e^{-(\nu\mu(t))\cdot dt})$$

where *B*(*n*,*p*) denotes a binomial distribution with *n* trials each with probability of success *p*. $F_{a,r}$ denotes the force of infection for individuals in age group a and risk group r and is given by

$$F_{a,r}(t) = \sum_{i\in A}\sum_{j\in K}(I^Y_{i,r}(t)\omega^Y + I^A_{i,r}(t)\omega^A + P^Y_{i,j}(t)\omega^{PY} + P^A_{i,j}(t)\omega^{PA})\beta(t)\phi_{a,i}/N_i$$

with

$$\beta(t) = e^{\log(\beta(0)) + b_1(t)\cdot PC1 + b_2(t)\cdot PC2 + Z(t)}$$

$$b_1(t) \sim N(b_1(t-1), \sigma_{b_1})$$
$$b_2(t) \sim N(b_2(t-1), \sigma_{b_2})$$
$$Z(t) \sim N(0.97 \cdot Z(t-1), \sigma_Z),\ Z(0) = 0.$$

where PC1 and PC2 describe the first and second principal components from our mobility data as described below. Finally,

$\mu(t) = e^{\log(\mu(0))+Z_\mu}$ where $Z_\mu(t) \sim N(\psi_\mu \cdot Z_\mu(t-1), \sigma_\mu),\ Z_\mu(0) = 0$ and

$\gamma^H(t) = e^{\log(\gamma^H(0))+Z_\gamma}$ where $Z_\gamma(t) \sim N(0.99 \cdot Z_\gamma(t-1), \sigma_\gamma),\ Z\gamma(0) = 0.$

We estimate $\beta(t)$, k, σ_Z, $b_1(t)$, $b_2(t)$, σ_{b_1}, σ_{b_2}, ψ_μ, σ_μ, and σ_γ as described in the model fitting section below.

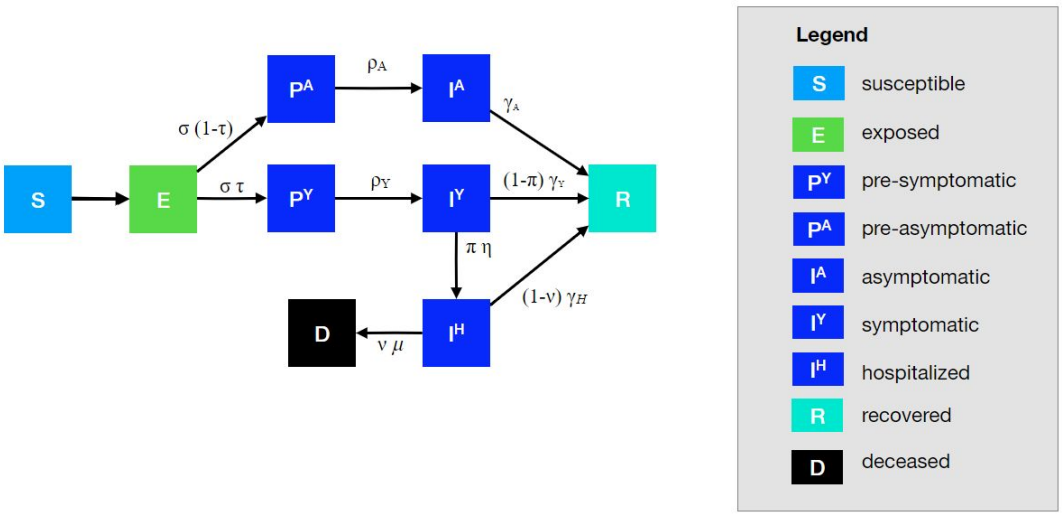

Figure A1. Compartmental model of COVID-19 transmission in the Austin MSA. Each subgroup (defined by age and risk) is modeled with a separate set of compartments. Upon infection, susceptible individuals (*S*) progress to exposed (*E*) and then to either pre-symptomatic infectious (P^Y) or pre-asymptomatic infectious (P^A) from which they move to symptomatic infectious (I^Y) and asymptomatic infectious (I^A) respectively. All asymptomatic cases eventually progress to a recovered class where they remain protected from future infection (*R*); symptomatic cases are either hospitalized (I^H) or recover. Mortality (*D*) varies by age group and risk group and is assumed to be preceded by hospitalization.

Mobility trends

We used mobility trends data from the Austin MSA to inform the transmission rate in our model. Specifically, we ran a principal component analysis (PCA) on eight independent mobility variables provided by SafeGraph, including home dwell time and visits to universities, bars, grocery stores, museums and parks, medical facilities, schools, and restaurants [3]. We regressed the transmission rate on the first two principal components from the mobility data as described in the modeling equations for $\beta(t)$.

Epidemic starting conditions

We could not estimate the epidemic start date directly using our model, because the transmission rate flexibility gave rise to similarly good fits within a wide-range of potential values for t_0. We therefore conducted an independent estimation procedure to obtain reasonable epidemic start dates for Austin. We then used our best guess parameters as described in Table A2 and chose $\beta(0) = 0.67$ as it produced three-day doubling rate in cumulative cases and gave $R_t(0) = 4$ which are consistent with observations for the Austin early outbreak dynamics [4]. We ran 1,000 stochastic simulations with these initial conditions, and identified the wait time for when there was 1 admit for Austin. We estimated the start time from the resulting distribution of wait times for Austin as February 17, 2020 (IQR = February 11 - February 23), and chose February 17th, 2020 as the start date for the model.

Model likelihood

We obtained daily hospital admit ($H_A(t)$), discharge data ($H_L(t)$), total hospitalizations ($H(t)$), and death data ($H_D(t)$) for the Austin MSA. In this model we estimated $\beta(t)$, k, σ_Z, $b_1(t)$, $b_2(t)$, σ_{b_1}, σ_{b_2}, ψ_μ, σ_μ, σ_γ and fixed the remaining parameters as described in Table A1-2. We assumed all sources of data were negative binomially distributed around their predicted values from the SEIR stochastic model, and chose informative, but relatively dispersed priors for certain parameters for stability in parameter estimation and to prevent the model from overfitting data through large perturbations to time-dependent variables.

Following all of these considerations, the likelihood for our stochastic model was:

$$p(Y(t), b_1(0), \sigma_{b_1}, b_2(0), \sigma_{b_2}, k|\theta) = p(Y(t)|\theta, b_1(0), \sigma_{b_1}, b_2(0), \sigma_{b_2}, k) \cdot p(\theta, b_1(0), \sigma_{b_1}, b_2(0), \sigma_{b_2}, k)$$

where $Y(t)$ refers to the four types of data from hospitals, θ contains all parameters from Table A1 not explicitly listed, and where

$$p(Y(t)|\theta, b_1(0), \sigma_{b_1}, b_2(0), \sigma_{b_2}, k) = p(H_A(t)|\hat{H}_A(t))p(H_L(t)|\hat{H}_L(t))p(H_D(t)|\hat{H}_D(t))p(H(t)|\hat{H}(t))$$
$$p(\theta, b_1(0), \sigma_{b_1}, b_2(0), \sigma_{b_2}, k) = p(b_1(0)) \cdot p(\sigma_{b_1}) \cdot p(b_2(0)) \cdot p(\sigma_{b_2}) \cdot p(k)$$

with

$$p(H_A(t)|\hat{H}_A(t)) = \binom{k + H_A(t) - 1}{H_A(t)} \cdot p^k (1-p)^{H_A(t)}, \text{ and } p = \frac{k}{k + \hat{H}_A(t)}$$
$$p(H_L(t)|\hat{H}_L(t)) = \binom{k + H_L(t) - 1}{H_L(t)} \cdot p^k (1-p)^{H_L(t)}, \text{ and } p = \frac{k}{k + \hat{H}_L(t)}$$
$$p(H_D(t)|\hat{H}_D(t)) = \binom{k + H_D(t) - 1}{H_D(t)} \cdot p^k (1-p)^{H_D(t)}, \text{ and } p = \frac{k}{k + \hat{H}_D(t)}$$

$$p(H(t)|\hat{H}(t)) = \binom{k + H(t) - 1}{H(t)} \cdot p^k (1-p)^{H(t)}, \text{ and } p = \frac{k}{k + \hat{H}(t)}$$

$$p(b_1(0)) \cdot t_d = \frac{1}{\sqrt{2}} e^{-\frac{1}{2}(\hat{b}_1(0))^2}$$

$$p(b_2(0)) \cdot t_d = \frac{1}{\sqrt{2}} e^{-\frac{1}{2}(\hat{b}_2(0))^2}$$

$$p(\sigma_{b_1}) \cdot t_d = \frac{1}{\Gamma(1.1) \cdot \frac{1}{1.1}^{1.1}} \hat{\sigma}_{b_1}^{1.1-1} e^{-1.1 \cdot \hat{\sigma}_{b_1}}$$

$$p(\sigma_{b_2}) \cdot t_d = \frac{1}{\Gamma(1.1) \cdot \frac{1}{1.1}^{1.1}} \hat{\sigma}_{b_2}^{1.1-1} e^{-1.1 \cdot \hat{\sigma}_{b_2}}$$

$$p(k) \cdot t_d = e^{\hat{k}}$$

and t_d is the number of days in the fitting time period.

Fitting method

In this model we estimated $\beta(t)$, k, σ_Z, $b_1(t)$, $b_2(t)$, σ_{b_1}, σ_{b_2}, ψ_μ, σ_μ, σ_γ and fixed the remaining parameters as described in Table A1. Fitting was carried out using the iterated filtering algorithm made available through the mif2 function in the pomp package in R [5,6]. This algorithm is a stochastic optimization procedure; it performs maximum likelihood estimation using a particle filter to provide a noisy estimate of the likelihood for a given combination of the parameters. For each parameter combination we ran 1,000 iterations of iterated filtering, each with 10,000 particles. We calculated smoothed posterior estimates for all of the states within the model through time (including $\beta(t)$ and other time-dependent parameters which are technically state variables in our model formulation, as it changes through time according to a stochastic process). We calculated these smoothed posteriors as follows:

1. We ran 1,000 independent particle filters at the MLE, each with 10,000 particles. For each run, l, of particle filtering, we kept track of the complete trajectory of each particle, as well as the filtered estimate of the likelihood, L_l.

2. For each of the 1,000 particle filtering runs, we randomly sampled a single complete particle trajectory, giving us 1,000 separate trajectories for all state variables.

3. We resampled from these trajectories with probabilities proportional to L_l to give a distribution of state trajectories

The result can be thought of as an empirical-Bayes posterior distribution: that is, a set of 1,000 smoothed posterior draws from all state variables, conditional on the maximum likelihood estimates for the model's free parameters. This smoothed posterior distribution is how we calculate means and credible intervals for $\beta(t)$ in addition to all other time-varying state variables.

Table A1. Model parameters[a]

Parameters	Value	Source
Start date	February 17, 2020	Estimated
Initial infections	1 symptomatic case age 18-49y	Assumption
$\beta(t)$: daily transmission rate	N/A	Estimated
γ^A: recovery rate on asymptomatic compartment	Equal to γ^Y	Assumption
γ^Y: recovery rate on symptomatic non-treated compartment	0.25	He et al. [7]
τ: symptomatic proportion (%)	57	Fox et al. [8]
σ: exposed rate	1/2.9	Zhang et al. [9]; He et al. [7]
ρ^A: pre-asymptomatic rate	Equal to ρ^Y	
ρ^Y: pre-symptomatic rate	$\frac{1}{2.3}$	He et al. [7]
P: proportion of pre-symptomatic transmission	44%	He et al. [7]
ω^P: relative infectiousness of pre-symptomatic individuals	$\omega^P = \frac{P}{1-P}\frac{\tau\omega^Y[YHR/\eta+(1-YHR)/\gamma^Y]+(1-\tau)\omega^A/\gamma^A}{\tau\omega^Y/\rho^Y+(1-\tau)\omega^A/\rho^A}$ $\omega^{PY} = \omega^P\omega^Y, \omega^{PA} = \omega^P\omega^A$	
ω^A: relative infectiousness of infectious individuals in compartment I^A	$\frac{2}{3}$	He et al. [10]
IFR: infected fatality ratio, age specific (%)	Low risk: [0.0009, 0.0022, 0.0339, 0.2520, 0.6440] High risk: [0.0092, 0.0218, 0.3388, 2.5197, 6.4402]	Age adjusted from Verity et al. [11]
YFR: symptomatic fatality ratio, age specific (%)	Low risk: [0.001608, 0.003823, 0.05943, 0.4420, 1.130] High risk: [0.01608, 0.03823, 0.5943, 4.420, 11.30]	$YFR = \frac{IFR}{\tau}$

h: high-risk proportion, age specific (%)	[8.2825, 14.1121, 16.5298, 32.9912, 47.0568]	Estimated using 2015-2016 Behavioral Risk Factor Surveillance System (BRFSS) data with multilevel regression and poststratification using CDC's list of conditions that may increase the risk of serious complications from influenza [12–14]

[a]Values given as five-element vectors are age-stratified with values corresponding to 0-4, 5-17, 18-49, 50-64, 65+ year age groups, respectively.

Table A2 Hospitalization parameters

Parameters	Value	Source
$\gamma^H(t)$: recovery rate in hospitalized compartment	Fitted	
YHR: symptomatic case hospitalization rate (%)	Low risk: [0.04021, 0.03091, 1.903, 4.114, 4.879] High risk: [0.4021, 0.3091, 19.03, 41.14, 48.79]	Age adjusted from Verity et al. [11]
π: rate of symptomatic individuals go to hospital, age-specific	$\pi = \frac{\gamma^Y * YHR}{\eta + (\gamma^Y - \eta)YHR}$	
η: rate from symptom onset to hospitalized	0.1695	5.9 day average from symptom onset to hospital admission Tindale et al. [15]
$\mu(t)$: rate from hospitalized to death	Fitted	
HFR: hospitalized fatality ratio, age specific (%)	[4, 12.365, 3.122, 10.745, 23.158]	$HFR = \frac{IFR}{\tau}$
ν: death rate on hospitalized individuals, age specific	$\nu = \frac{\gamma^H HFR}{\mu + (\gamma^H - \mu)HFR}$	
ICU: proportion hospitalized people in ICU	0.35	Estimated from Austin COVID-19 hospitalization data

Table A3 Contact matrix. Daily number contacts by age group on an average day.

	0-4y	5-17y	18-49y	50-64y	65y+
0-4y	1.88	2.02	4.01	0.79	0.28
5-17y	0.55	7.06	5.02	0.70	0.22
18-49y	0.37	2.19	8.72	1.45	0.21
50-64y	0.33	1.62	5.79	2.79	0.50
65y+	0.19	0.88	2.36	1.19	1.22

Estimation of age-stratified proportion of population at high-risk for COVID-10 complications

We estimate age-specific proportions of the population at high risk of complications from COVID-19 based on data for Austin, TX and Round-Rock, TX from the CDC's 500 cities project (Figure A2) [16]. We assume that high risk conditions for COVID-19 are the same as those specified for influenza by the CDC [12]. The CDC's 500 cities project provides city-specific estimates of prevalence for several of these conditions among adults [17]. The estimates were obtained from the 2015-2016 Behavioral Risk Factor Surveillance System (BRFSS) data using a small-area estimation methodology called multi-level regression and poststratification [13,14]. It links geocoded health surveys to high spatial resolution population demographic and socioeconomic data [14].

Estimating high-risk proportions for adults. To estimate the proportion of adults at high risk for complications, we use the CDC's 500 cities data, as well as data on the prevalence of HIV/AIDS, obesity and pregnancy among adults (Table A6).

The CDC 500 cities dataset includes the prevalence of each condition on its own, rather than the prevalence of multiple conditions (e.g., dyads or triads). Thus, we use separate co-morbidity estimates to determine overlap. Reference about chronic conditions [18] gives US estimates for the proportion of the adult population with 0, 1 or 2+ chronic conditions, per age group. Using this and the 500 cities data we can estimate the proportion of the population p_{HR} in each age group in each city with at least one chronic condition listed in the CDC 500 cities data (Table A6) putting them at high-risk for flu complications.

HIV: We use the data from table 20a in CDC HIV surveillance report [19] to estimate the population in each risk group living with HIV in the US (last column, 2015 data). Assuming independence between HIV and other chronic conditions, we increase the proportion of the population at high-risk for influenza to account for individuals with HIV but no other underlying conditions.

Morbid obesity: A BMI over 40kg/m^2 indicates morbid obesity, and is considered high risk for influenza. The 500 Cities Project reports the prevalence of obese people in each city with BMI over 30kg/m^2 (not necessarily morbid obesity). We use the data from table 1 in Sturm and Hattori [20] to estimate the proportion of people with BMI>30 that actually have BMI>40 (across the US); we then apply this to the 500 Cities obesity data to estimate the proportion of people who are morbidly obese in each city. Table 1 of Morgan et al. [21] suggests that 51.2% of morbidly obese adults have at least one other high risk chronic condition, and update our high-risk population estimates accordingly to account for overlap.

Pregnancy: We separately estimate the number of pregnant women in each age group and each city, following the methodology in CDC reproductive health report [22]. We assume independence between any of the high-risk factors and pregnancy, and further assume that half the population are women.

Estimating high-risk proportions for children. Since the 500 Cities Project only reports data for adults 18 years and older, we take a different approach to estimating the proportion of children at high risk for severe influenza. The two most prevalent risk factors for children are asthma and obesity; we also account for childhood diabetes, HIV and cancer.
From Miller et al. [23], we obtain national estimates of chronic conditions in children. For asthma, we assume that variation among cities will be similar for children and adults. Thus, we use the relative prevalences of asthma in adults to scale our estimates for children in each city. The prevalence of HIV and cancer in children are taken from CDC HIV surveillance report [19] and cancer research report [24], respectively.

We first estimate the proportion of children having either asthma, diabetes, cancer or HIV (assuming no overlap in these conditions). We estimate city-level morbid obesity in children using the estimated morbid obesity in adults multiplied by a national constant ratio for each age group estimated from Hales et al. [25], this ratio represents the prevalence in morbid obesity in children given the one observed in adults. From Morgan et al. [21], we estimate that 25% of morbidly obese children have another high-risk condition and adjust our final estimates accordingly.

Resulting estimates. We compare our estimates for the Austin-Round Rock Metropolitan Area to published national-level estimates [26] of the proportion of each age group with underlying high risk conditions (Table A6). The biggest difference is observed in older adults, with Austin having a lower proportion at risk for complications for COVID-19 than the national average; for 25-39 year olds the high risk proportion is slightly higher than the national average.

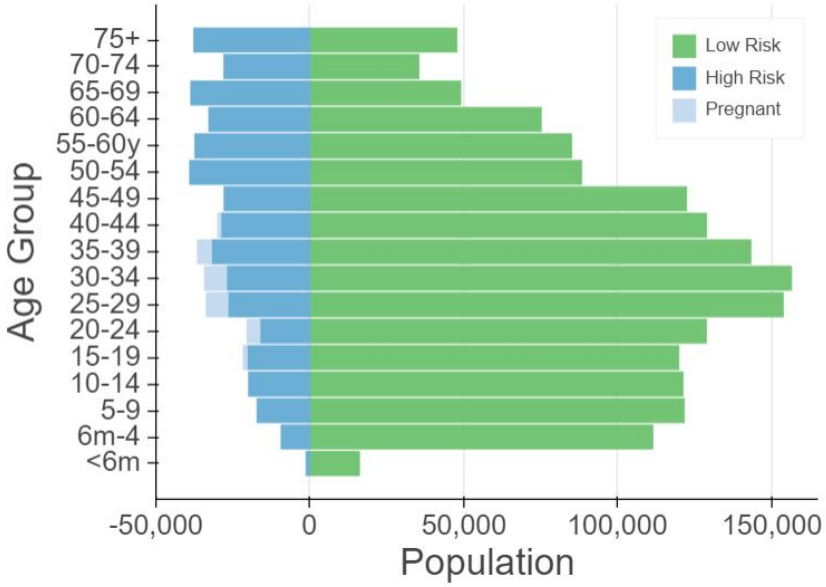

Figure A2. Demographic and risk composition of the Austin-Round Rock MSA. Bars indicate age-specific population sizes, separated by low risk, high risk, and pregnant. High risk is defined as individuals with cancer, chronic kidney disease, COPD, heart disease, stroke, asthma, diabetes, HIV/AIDS, and morbid obesity, as estimated from the CDC 500 Cities Project [16], reported HIV prevalence [19] and reported morbid obesity prevalence [20,21], corrected for multiple conditions. The population of pregnant women is derived using the CDC's method combining fertility, abortion and fetal loss rates [27–29].

Table A4. High-risk conditions for influenza and data sources for prevalence estimation

Condition	Data source
Cancer (except skin), chronic kidney disease, COPD, coronary heart disease, stroke, asthma, diabetes	CDC 500 cities [16]
HIV/AIDS	CDC HIV Surveillance report [19]
Obesity	CDC 500 cities [16], Sturm and Hattori [20], Morgan et al. [21]
Pregnancy	National Vital Statistics Reports [27] and abortion data [28]

Table A5. Comparison between published national estimates and Austin-Round Rock MSA estimates of the percent of the population at high-risk of influenza/COVID-19 complications.

Age Group	National estimates [25]	Austin-Round Rock (excluding pregnancy)	Pregnant women (proportion of age group)
0 to 6 months	NA	8.1	-
6 months to 4 years	6.8	9.0	-
5 to 9 years	11.7	14.6	-
10 to 14 years	11.7	16.7	-
15 to 19 years	11.8	17.0	3.2
20 to 24 years	12.4	13.2	10.6
25 to 34 years	15.7	17.4	9.6
35 to 39 years	15.7	22.1	3.7
40 to 44 years	15.7	22.5	0.6
45 to 49 years	15.7	22.7	-
50 to 54 years	30.6	37.5	-
55 to 60 years	30.6	37.4	-
60 to 64 years	30.6	37.3	-
65 to 69 years	47.0	53.2	-
70 to 74 years	47.0	53.2	-
75 years and older	47.0	53.2	-

References

1. Seventh Amended Emergency Order for Public Health Emergency due to COVID-19. [cited 28 Apr 2020]. Available: https://co.jefferson.tx.us/documents/Coronavirus%20Docs/coronavirusdocs.htm

1. Keeling MJ, Rohani P. Modeling Infectious Diseases in Humans and Animals. Princeton University Press; 2011.

2. Gillespie DT. Approximate accelerated stochastic simulation of chemically reacting systems. J Chem Phys. 2001;115: 1716–1733.

3. Gao S, Rao J, Kang Y, Liang Y, Kruse J. Mapping county-level mobility pattern changes in

the United States in response to COVID-19. arXiv [physics.soc-ph]. 2020. Available: http://arxiv.org/abs/2004.04544

4. Liu Y, Gayle AA, Wilder-Smith A, Rocklöv J. The reproductive number of COVID-19 is higher compared to SARS coronavirus. J Travel Med. 2020;27. doi:10.1093/jtm/taaa021

5. R Core Team. R: A Language and Environment for Statistical Computing. Vienna, Austria: R Foundation for Statistical Computing; 2020. Available: https://www.R-project.org/

6. King AA, Nguyen D, Ionides EL. Statistical Inference for Partially Observed Markov Processes via the R Package pomp. arXiv [stat.ME]. 2015. Available: http://arxiv.org/abs/1509.00503

7. He X, Lau EHY, Wu P, Deng X, Wang J, Hao X, et al. Temporal dynamics in viral shedding and transmissibility of COVID-19. Nat Med. 2020. doi:10.1038/s41591-020-0869-5

8. Fox SJ, Pasco R, Tec M, Du Z, Lachmann M, Scott J, et al. The impact of asymptomatic COVID-19 infections on future pandemic waves. medRxiv. 2020. Available: https://www.medrxiv.org/content/10.1101/2020.06.22.20137489v1.abstract

9. Zhang J, Litvinova M, Wang W, Wang Y, Deng X, Chen X, et al. Evolving epidemiology and transmission dynamics of coronavirus disease 2019 outside Hubei province, China: a descriptive and modelling study. Lancet Infect Dis. 2020. doi:10.1016/S1473-3099(20)30230-9

10. He D, Zhao S, Lin Q, Zhuang Z, Cao P, Wang MH, et al. The relative transmissibility of asymptomatic COVID-19 infections among close contacts. Int J Infect Dis. 2020;94: 145–147.

11. Verity R, Okell LC, Dorigatti I, Winskill P, Whittaker C, Imai N, et al. Estimates of the severity of COVID-19 disease. Epidemiology. medRxiv; 2020. doi:10.1101/2020.03.09.20033357

12. CDC. People at High Risk of Flu. In: Centers for Disease Control and Prevention [Internet]. 1 Nov 2019 [cited 26 Mar 2020]. Available: https://www.cdc.gov/flu/highrisk/index.htm

13. CDC - BRFSS. 5 Nov 2019 [cited 26 Mar 2020]. Available: https://www.cdc.gov/brfss/index.html

14. Zhang X, Holt JB, Lu H, Wheaton AG, Ford ES, Greenlund KJ, et al. Multilevel regression and poststratification for small-area estimation of population health outcomes: a case study of chronic obstructive pulmonary disease prevalence using the behavioral risk factor surveillance system. Am J Epidemiol. 2014;179: 1025–1033.

15. Tindale L, Coombe M, Stockdale JE, Garlock E, Lau WYV, Saraswat M, et al. Transmission interval estimates suggest pre-symptomatic spread of COVID-19. Epidemiology. medRxiv; 2020. doi:10.1101/2020.03.03.20029983

16. 500 Cities Project: Local data for better health | Home page | CDC. 5 Dec 2019 [cited 19 Mar 2020]. Available: https://www.cdc.gov/500cities/index.htm

17. Health Outcomes | 500 Cities. 25 Apr 2019 [cited 28 Mar 2020]. Available: https://www.cdc.gov/500cities/definitions/health-outcomes.htm

18. Part One: Who Lives with Chronic Conditions. In: Pew Research Center: Internet, Science & Tech [Internet]. 26 Nov 2013 [cited 23 Nov 2019]. Available: https://www.pewresearch.org/internet/2013/11/26/part-one-who-lives-with-chronic-conditions/

19. for Disease Control C, Prevention, Others. HIV surveillance report. 2016; 28. URL: http://www cdc gov/hiv/library/reports/hiv-surveil-lance html Published November. 2017.

20. Sturm R, Hattori A. Morbid obesity rates continue to rise rapidly in the United States. Int J Obes . 2013;37: 889–891.

21. Morgan OW, Bramley A, Fowlkes A, Freedman DS, Taylor TH, Gargiullo P, et al. Morbid obesity as a risk factor for hospitalization and death due to 2009 pandemic influenza A(H1N1) disease. PLoS One. 2010;5: e9694.

22. Estimating the Number of Pregnant Women in a Geographic Area from CDC Division of Reproductive Health. Available: https://www.cdc.gov/reproductivehealth/emergency/pdfs/PregnacyEstimatoBrochure508.pdf

23. Miller GF, Coffield E, Leroy Z, Wallin R. Prevalence and Costs of Five Chronic Conditions in Children. J Sch Nurs. 2016;32: 357–364.

24. Cancer Facts & Figures 2014. [cited 30 Mar 2020]. Available: https://www.cancer.org/research/cancer-facts-statistics/all-cancer-facts-figures/cancer-facts-figures-2014.html

25. Hales CM, Fryar CD, Carroll MD, Freedman DS, Ogden CL. Trends in Obesity and Severe Obesity Prevalence in US Youth and Adults by Sex and Age, 2007-2008 to 2015-2016. JAMA. 2018;319: 1723–1725.

26. Zimmerman RK, Lauderdale DS, Tan SM, Wagener DK. Prevalence of high-risk indications for influenza vaccine varies by age, race, and income. Vaccine. 2010;28: 6470–6477.

27. Martin JA, Hamilton BE, Osterman MJK, Driscoll AK, Drake P. Births: Final Data for 2017. Natl Vital Stat Rep. 2018;67: 1–50.

28. Jatlaoui TC, Boutot ME, Mandel MG, Whiteman MK, Ti A, Petersen E, et al. Abortion Surveillance - United States, 2015. MMWR Surveill Summ. 2018;67: 1–45.

29. Ventura SJ, Curtin SC, Abma JC, Henshaw SK. Estimated pregnancy rates and rates of pregnancy outcomes for the United States, 1990-2008. Natl Vital Stat Rep. 2012;60: 1–21.

Appendix 2: Determining Triggers for Launching an Alternate Care Site (ACS)

ACS Optimization Model

To find thresholds for triggering an alternate care site (ACS), we form a stochastic optimization model, in which disease dynamics are characterized by an enhanced SEIR-style model of disease transmission [1]. This epidemiological model comprises compartments for susceptible, exposed, pre-asymptomatic, pre-symptomatic, infectious-asymptomatic, infectious-symptomatic, infected and hospitalized in the general ward, infected and hospitalized in the intensive care unit (ICU), recovered, and deceased, which we denote by S, E, PA, PY, IA, IY, IH, ICU, R, and D, respectively. Fig. 1 diagrams the model's compartments and transitions for a metropolitan area. The population is partitioned into ten groups consisting of five age groups of low-risk and another five of high-risk individuals. Each group is represented with its own set of ten compartments (susceptible, exposed, etc.) so that in total the epidemiological model has 100 compartments.

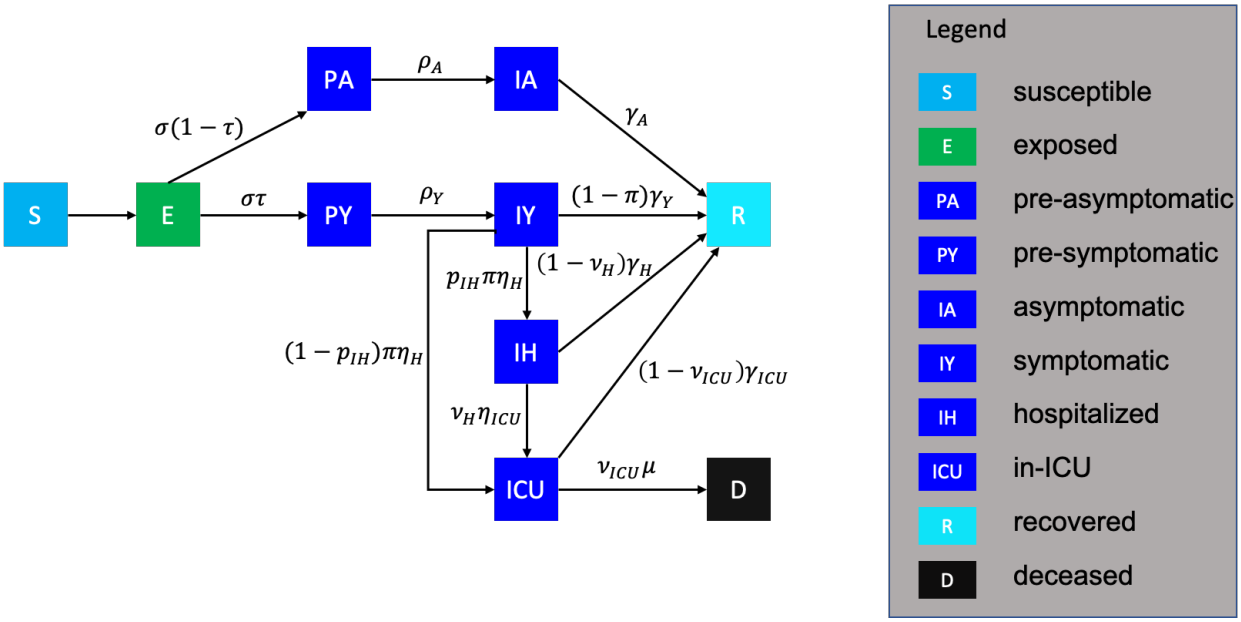

Figure 1: Diagram of the epidemiological model with compartments, transitions, and rates. The model has ten copies of such diagrams for each age-risk group pair, which interact to determine the (unmarked) rate of transition from compartment S to E. Such transitions are governed by the transmission rate β but also time-dynamic contact matrices.

Given our estimates of the time-dynamic contact matrices, which change with weekdays versus weekends, whether schools are open, and other pandemic-related changes in the community's behavior, we can use the stochastic SEIR model described below to estimate peak hospitalization demand. Given existing COVID-19 hospital capacity, B, we let $B + B_{ACS}$ denote the 95th percentile of the peak hospitalization demand rounded to 50 beds; i.e., we size the ACS so that we are at least 95% confident that its capacity will not be exceeded and we assume the ACS operates for T_{ACS} days. Given this, we monitor the seven-day moving average of new COVID-19 hospital admissions, and we optimize a threshold, denoted by ℓ, such that when the seven-day average exceeds ℓ we stand up the ACS so it is operational 14 days later. By maximizing ℓ we

delay, as long as possible, ACS construction while employing a probabilistic constraint to ensure the system does not exceed capacity with probability 0.95. In particular, we use Monte Carlo simulation to form a set of scenarios, indexed by ω, and use binary variables to count the number of paths that violate capacity at any point in time.

Notation:

Indices and Sets

$t \in \mathcal{T}$	set of time periods $\{1, 2, \ldots, \lvert\mathcal{T}\rvert\}$ [day]
$t \in \mathcal{T}_0$	$\mathcal{T} \cup \{0\}$
$a \in \mathcal{A}$	set of age groups {0-4y, 5-17y, 18-49y, 50-64y, 65y+}
$r \in \mathcal{R}$	risk groups $\{low, high\}$
$i \in \mathcal{I}$	predefined stages of transmission that affect contact matrices ($\phi_{i,t}^{a',r',a,r}$ below); we use $\mathcal{I} = \{1\,(\text{red}), 2\,(\text{orange}), 3\,(\text{yellow}), 4\,(\text{blue})\}$
$\omega \in \Omega$	set of scenarios

Parameters

Epidemiological parameters:

β	unmitigated transmission rate
σ	rate at which exposed individuals become infectious
τ	proportion of exposed individuals who become symptomatic
ρ_A	rate at which pre-asymptomatic individuals become asymptomatic
ρ_Y	rate at which pre-symptomatic individuals become symptomatic
γ_A	recovery rate from asymptomatic compartment
γ_Y	recovery rate from symptomatic compartment
γ_H^a	recovery rate from hospitalized compartment for age group a
γ_{ICU}^a	recovery rate from ICU compartment for age group a
P	proportion of pre-symptomatic transmission
$YHR^{a,r}$	percent of symptomatic infectious that go to the hospital for age-risk group a, r
η_H	hospitalization rate after symptom onset
ω_A	infectiousness of individuals in IA relative to IY
$\omega_P^{a,r}$	$\frac{P}{1-P}\frac{\tau(YHR^{a,r}/\eta_H+(1-YHR^{a,r})/\gamma_Y)+(1-\tau)\omega_A/\gamma_A}{\tau/\rho_Y+(1-\tau)\omega_A/\rho_A}$: infectiousness of pre-symptomatic individuals relative to IY for age-risk group a, r
$\pi^{a,r}$	$\frac{\gamma_Y \cdot YHR^{a,r}}{[\eta_H-(\eta_H-\gamma_Y)YHR^{a,r}]}$: rate-adjusted proportion of symptomatic individuals who go to the hospital for age-risk group a, r
p_{IH}	percent of patients directly going to the general ward of the hospital
$HICUR$	percent of general ward patients who get transferred to ICU
η_{ICU}^a	ICU admission rate after admission to the general ward for age group a
ν_H^a	$\frac{\gamma_H^a \cdot HICUR}{[\eta_{ICU}^a-(\eta_{ICU}^a-\gamma_H^a)HICUR]}$: rate-adjusted proportion of general ward patients transferred to ICU for age group a
μ^a	rate from ICU to death for age group a
$ICUFR^a$	percent of hospitalized that die for age group a
ν_{ICU}^a	$\frac{\gamma_{ICU}^a \cdot ICUFR^a}{[\mu^a-(\mu^a-\gamma_{ICU}^a)ICUFR^a]}$: ICU fatality rate-adjusted proportion for age group a
$\phi_{i,t}^{a',r',a,r}$	expected number of daily contacts from (a', r') to (a, r) at time t under stage i
$X_{i,t,\omega}$	1 if system is in stage i at t for ω, 0 otherwise; estimated via hospitalization data

$N^{a,r}$	population of age-risk group a, r
Additional parameters:	
B	number of hospital beds, including general ward and ICU, for COVID-19 patients
B_{ACS}	ACS bed capacity for COVID-19 patients
T_{ACS}	length of operational ACS for COVID-19 patients
ε	violation probability for probabilistic constraint, e.g., $\varepsilon = 0.05$

Variables

Epidemiological variables (for scenario $\omega \in \Omega$):	
$S^{a,r}_{t,\omega}$	number of susceptible people of age group a, risk group r at time t [persons]
$dS^{a,r}_{t,\omega}$	$S^{a,r}_{t,\omega} - S^{a,r}_{t+1,\omega}$ [persons]
$E^{a,r}_{t,\omega}$	number of exposed people of age group a, risk group r at time t [persons]
$PA^{a,r}_{t,\omega}$	number of pre-asymptomatic people for a, r, t [persons]
$PY^{a,r}_{t,\omega}$	number of pre-symptomatic people for a, r, t [persons]
$IA^{a,r}_{t,\omega}$	number of infectious-asymptomatic people for a, r, t [persons]
$IY^{a,r}_{t,\omega}$	number of infectious-symptomatic people for a, r, t [persons]
$IH^{a,r}_{t,\omega}$	number of infected-hospitalized people in the general ward for a, r, t [persons]
$ICU^{a,r}_{t,\omega}$	number of infected-hospitalized people in the ICU for a, r, t [persons]
$R^{a,r}_{t,\omega}$	number of recovered people for a, r, t [persons]
$D^{a,r}_{t,\omega}$	number of deceased people for a, r, t [persons]
$H_{t,\omega}$	daily hospital admissions, from infectious-symptomatic to the general ward and ICU, at time t [persons/day]
$\overline{H}_{t,\omega}$	seven-day moving average of $H_{t,\omega}$ [persons/day]
$U_{t,\omega}$	daily ICU admissions (from infectious-symptomatic and the general ward) at time t [persons/day]
Intervention variables:	
ℓ	the threshold (level) for the daily hospitalization rate
Z_ω	1 if healthcare capacity is exceeded in scenario ω; 0 otherwise

We refer to Table 7 for further details on model parameters. We first define the epidemiological transition dynamics in the following equations for all $\omega \in \Omega$:

$$S^{a,r}_{t+1,\omega} - S^{a,r}_{t,\omega} = -dS^{a,r}_{t,\omega} \qquad \forall t \in \mathcal{T}_0, a \in \mathcal{A}, r \in \mathcal{R} \quad [1a]$$

$$E^{a,r}_{t+1,\omega} - E^{a,r}_{t,\omega} = dS^{a,r}_{t,\omega} - \sigma E^{a,r}_{t,\omega} \qquad \forall t \in \mathcal{T}_0, a \in \mathcal{A}, r \in \mathcal{R} \quad [1b]$$

$$PA^{a,r}_{t+1,\omega} - PA^{a,r}_{t,\omega} = \sigma(1-\tau)E^{a,r}_{t,\omega} - \rho_A PA^{a,r}_{t,\omega} \qquad \forall t \in \mathcal{T}_0, a \in \mathcal{A}, r \in \mathcal{R} \quad [1c]$$

$$IA^{a,r}_{t+1,\omega} - IA^{a,r}_{t,\omega} = \rho_A PA^{a,r}_{t,\omega} - \gamma_A IA^{a,r}_{t,\omega} \qquad \forall t \in \mathcal{T}_0, a \in \mathcal{A}, r \in \mathcal{R} \quad [1d]$$

$$PY^{a,r}_{t+1,\omega} - PY^{a,r}_{t,\omega} = \sigma\tau E^{a,r}_{t,\omega} - \rho_Y PY^{a,r}_{t,\omega} \qquad \forall t \in \mathcal{T}_0, a \in \mathcal{A}, r \in \mathcal{R} \quad [1e]$$

$$IY^{a,r}_{t+1,\omega} - IY^{a,r}_{t,\omega} = \rho_Y PY^{a,r}_{t,\omega} - (1-\pi^{a,r})\gamma_Y IY^{a,r}_{t,\omega} - \pi^{a,r}\eta_H IY^{a,r}_{t,\omega} \qquad \forall t \in \mathcal{T}_0, a \in \mathcal{A}, r \in \mathcal{R} \quad [1f]$$

$$IH^{a,r}_{t+1,\omega} - IH^{a,r}_{t,\omega} = p_{IH}\pi^{a,r}\eta_H IY^{a,r}_{t,\omega} - (1-\nu^a_H)\gamma^a_H IH^{a,r}_{t,\omega} - \nu^a_H\eta^a_{ICU} IH^{a,r}_{t,\omega} \qquad \forall t \in \mathcal{T}_0, a \in \mathcal{A}, r \in \mathcal{R} \quad [1g]$$

$$ICU^{a,r}_{t+1,\omega} - ICU^{a,r}_{t,\omega} = (1-p_{IH})\pi^{a,r}\eta_H IY^{a,r}_{t,\omega} + \nu^a_H\eta^a_{ICU} IH^{a,r}_{t,\omega} - \quad [1h]$$

$$(1-\nu^a_{ICU})\gamma^a_{ICU} ICU^{a,r}_{t,\omega} - \nu^a_{ICU}\mu^a ICU^{a,r}_{t,\omega} \qquad \forall t \in \mathcal{T}_0, a \in \mathcal{A}, r \in \mathcal{R} \quad [1i]$$

$$R^{a,r}_{t+1,\omega} - R^{a,r}_{t,\omega} = \gamma_A IA^{a,r}_{t,\omega} + (1-\pi^{a,r})\gamma_Y IY^{a,r}_{t,\omega} + (1-\nu^a_H)\gamma^a_H IH^{a,r}_{t,\omega} + \quad [1j]$$

$$(1-\nu^a_{ICU})\gamma^a_{ICU} ICU^{a,r}_{t,\omega} \qquad \forall t \in \mathcal{T}_0, a \in \mathcal{A}, r \in \mathcal{R} \quad [1k]$$

$$D^{a,r}_{t+1,\omega} - D^{a,r}_{t,\omega} = \nu^a_{ICU}\mu^a ICU^{a,r}_{t,\omega} \qquad \forall t \in \mathcal{T}_0, a \in \mathcal{A}, r \in \mathcal{R} \quad [1l]$$

$$dS^{a,r}_{t,\omega} = S^{a,r}_{t,\omega} \sum_{a' \in \mathcal{A}} \sum_{r' \in \mathcal{R}} \sum_{i \in \mathcal{I}} \frac{\beta \phi^{a',r',a,r}_{i,t} X_{i,t,\omega}}{N^{a',r'}} \left(IY^{a',r'}_t + \omega_A IA^{a',r'}_t + \right.$$

$$\left. \omega^{a',r'}_P \omega_A PA^{a',r'}_t + \omega^{a',r'}_P PY^{a',r'}_t \right) \qquad \forall t \in \mathcal{T}_0, a \in \mathcal{A}, r \in \mathcal{R}. \quad [1m]$$

The initial conditions, for analysis have all variables indexed by $t = 0$ as zero except the following:

$$IY^{\text{18-49},low}_{0,\omega} = 1, S^{\text{18-49},low}_{0,\omega} = N^{\text{18-49},low} - 1, \text{and } S^{a,r}_{0,\omega} = N_{a,r} \forall (a,r) \in \mathcal{A} \times \mathcal{R} \setminus \{(\text{18-49}, low)\}. \quad [2]$$

The epidemiological dynamics largely follow the formulation used in [2] with the addition of three compartments to improve model fidelity and to distinguish beds in the ICU and general ward. The initial conditions specify a single infectious individual in the 18-49 age group with low risk. The age-risk groups are initialized with the rest of the population in their respective susceptible compartments. Eqs. [1a]-[1m] then provide a sample path, indexed by ω, for the progression of the disease in the community. The indicator variables $X_{i,t,\omega} \in \{0,1\}$ are estimated and then taken as input, and select the current stage and, in turn, the expected number of daily contacts via $\phi^{a',r',a,r}_{i,t}$. These binary indicator variables satisfy $\sum_{i \in \mathcal{I}} X_{i,t,\omega} = 1$, i.e., we are in exactly one stage of transmission at any point in time, and they are estimated based on hospitalization data. While our notation allows them to depend on the sample path, ω, we use point estimates, which do not depend on ω in our implementation. The contact matrices are indexed by t because they capture whether school is currently open and if so, the school calendar; they further capture weekdays versus weekends and the level of cocooning, which can vary with time; and they capture contacts at school, home, work, and another catch-all category. We assume that sufficient precautions are taken in hospitals so that hospitalized cases do *not* contribute to infecting others via Eq. [1m]. The most significant updates of the model from that in [2] are in additional compartments. We use constructs similar to He et al. [3] for a pre-symptomatic period to more accurately model the profile of infectiousness of individuals by including pre-symptom onset transmission. We also model the ICU compartment explicitly for two reasons. First, patients in the ICU have different durations in the hospital than those in the general ward, and second it allows us to account for ICU capacity as a resource (although we do not do so explicitly here). We let p_{IH} denote the probability a hospitalized patient is admitted to a general ward bed and the remaining fraction go directly to the ICU. As

Fig. 1 and Eq. [1h] indicate, it is possible to transfer general ward patients to the ICU later if needed. All deaths are recorded from the ICU.

The stochastic optimization model can be formulated as follows:

$$\max \quad \ell \qquad [3a]$$

$$\text{s.t.} \quad \text{Equations [1] and [2]} \qquad [3b]$$

$$H_{t,\omega} = \sum_{a\in\mathcal{A}}\sum_{r\in\mathcal{R}} \pi^{a,r}\eta_H I Y^{a,r}_{t,\omega} \qquad \forall t \in \mathcal{T}, \omega \in \Omega \qquad [3c]$$

$$\overline{H}_{t,\omega} = \frac{1}{7}\sum_{t'=\max\{t-6,1\}}^{t} H_{t,\omega} \qquad \forall t \in \mathcal{T}, \omega \in \Omega \qquad [3d]$$

$$\sum_{a\in\mathcal{A}}\sum_{r\in\mathcal{R}} (ICU^{a,r}_{t,\omega} + IH^{a,r}_{t,\omega}) \le B + B_{ACS}\mathbb{I}_{ACS,t} + MZ_\omega \qquad \forall t \in \mathcal{T}, \omega \in \Omega \qquad [3e]$$

$$\sum_{\omega\in\Omega} Z_\omega \le \lfloor \varepsilon|\Omega| \rfloor \qquad [3f]$$

$$\ell \ge 0 \qquad [3g]$$

$$Z_\omega \in \{0,1\} \qquad \forall \omega \in \Omega. \qquad [3h]$$

For simplicity, we write the finite-difference Eqs. [1] in a deterministic form. They become stochastic, and require indexing by ω, because binomial random variables replace terms like $\sigma E^{a,r}_{t,\omega}$; here the binomial random variable has parameter $n = E^{a,r}_{t,\omega}$ and σ serves as the "success" probability. This construct is pervasive throughout right-hand side terms in Eqs. [1]. In addition to these "micro" stochastics there are "macro" stochastics because we model σ, ω_A, γ_A, and γ_Y as random variables that are subject to a Monte Carlo draw at time 0 of the simulation. We discuss this further below (Selection of Scenarios).

For each sample path, ω, we record the number of daily hospital admissions and its seven-day moving average in constraints [3c] and [3d], aggregated across the general ward and ICU. Constraint [3e] identifies scenarios for which, at some time point, the number of patients exceeds the capacity, where M is sufficiently large so the constraint is vacuous if $Z_\omega = 1$. Here, capacity is simply B if the ACS is not operational and is $B + B_{ACS}$ if it is operational. The indicator term, $\mathbb{I}_{ACS}$, takes value one if the ACS is in place and value zero otherwise:

$$\mathbb{I}_{ACS,t} = \begin{cases} 1 & \text{if } \overline{H}_{t-14,\omega} \ge \ell \text{ or } \exists t' \in [t - T_{ACS}, t], \text{s.t. } \mathbb{I}_{ACS,t'} - \mathbb{I}_{ACS,t'-1} = 1 \\ 0 & \text{otherwise.} \end{cases}$$

Constraint [3f] ensures the probability that a violation of capacity occurs is at most fraction ε of the total scenarios.

We have formulated the model with daily time periods, which simplifies notation for computing the seven-day moving average of new admissions, the logic behind taking two weeks for the ACS to become operational. That said, in implementation we use ten time steps per day, which suffices for the fidelity of the epidemiological dynamics in Eqs. [1].

We generate 300 scenarios for Ω according to the procedure described below (Selection of Scenarios). After obtaining a set of optimal triggers, we generate another 300 scenarios, Ω', to assess performance.

Those two sets of scenarios are similar to "training" and "testing" data used in statistics and machine learning. As a result, it is possible to obtain thresholds that meet the probabilistic constraint under Ω, but violate that constraint when tested using Ω', although in our experience such violations are both rare and modest.

Model [3] is a large-scale stochastic mixed-integer nonlinear program. Problems of the scale we consider cannot currently be solved using commercial integer programming software. We approximately solve the model using a grid search procedure. For a fixed threshold, ℓ, we can run the simulation model for all $\omega \in \Omega$ in parallel, applying transition dynamics [1]-[2] and using the logic of [3c]-[3e] to compute the binary variables which indicate the scenarios with capacity violations, Z_ω. For each threshold that we consider in our grid search, we select the configuration that yields the largest threshold, ℓ; i.e., we delay construction of the ACS as long as possible while satisfying the probabilistic constraint [3f]. Our grid search uses increments of 10 daily admissions. The model does not explicitly model closing of the ACS, but this is straightforward as discussed in the main text.

Model Parameters

Table 1 partitions the Austin MSA population based on age groups (0-4 years old, 5-17 years old, 18-49 years old, 50-64 years old, and 65 years and older) and risk groups (low risk and high risk). The high-risk group proportions are estimated based on the population with chronic conditions listed by the CDC 500 cities data [4]. Population data processing is detailed in the appendix of [2] and here we present only the final numbers used for this paper's analysis.

$N^{a,r}$	0-4	5-17	18-49	50-64	65 and older
Low risk	128527	327148	915894	249273	132505
High risk	9350	37451	156209	108196	103763

Table 1: Austin age-risk group populations.

We define four baseline contact matrices, $\mathcal{H}, \mathcal{S}, \mathcal{W}$, and $\mathcal{O}$, to describe the contact frequency between age groups at home, at school, at work, and at other locations. These *baseline* matrices assume there is no difference in contacts among the low- and high-risk groups. Each row and column represents an age group, in the order of 0-4 years old, 5-17 years old, 18-49 years old, 50-64 years old, and 65 years old and above, with the row-column value corresponding to a "from-to" transmission contact:

$$\mathcal{H} = \begin{bmatrix} 0.5 & 0.9 & 2.0 & 0.1 & 0.0 \\ 0.2 & 1.7 & 1.9 & 0.2 & 0.0 \\ 0.2 & 0.9 & 1.7 & 0.2 & 0.0 \\ 0.2 & 0.7 & 1.2 & 1.0 & 0.1 \\ 0.1 & 0.7 & 1.0 & 0.3 & 0.6 \end{bmatrix} \quad \mathcal{S} = \begin{bmatrix} 1.0 & 0.5 & 0.4 & 0.1 & 0.0 \\ 0.2 & 3.7 & 0.9 & 0.1 & 0.0 \\ 0.0 & 0.7 & 0.8 & 0.0 & 0.0 \\ 0.1 & 0.8 & 0.5 & 0.1 & 0.0 \\ 0.0 & 0.0 & 0.1 & 0.0 & 0.0 \end{bmatrix}$$

$$\mathcal{W} = \begin{bmatrix} 0.0 & 0.0 & 0.0 & 0.0 & 0.0 \\ 0.0 & 0.1 & 0.4 & 0.0 & 0.0 \\ 0.0 & 0.2 & 4.5 & 0.8 & 0.0 \\ 0.0 & 0.1 & 2.8 & 0.9 & 0.0 \\ 0.0 & 0.0 & 0.1 & 0.0 & 0.0 \end{bmatrix} \quad \mathcal{O} = \begin{bmatrix} 0.7 & 0.7 & 1.8 & 0.6 & 0.3 \\ 0.2 & 2.6 & 2.1 & 0.4 & 0.2 \\ 0.1 & 0.7 & 3.3 & 0.6 & 0.2 \\ 0.1 & 0.3 & 2.2 & 1.1 & 0.4 \\ 0.0 & 0.2 & 1.3 & 0.8 & 0.6 \end{bmatrix}.$$

The contact matrices $\phi_{i,t}^{a',r',a,r}$ are calculated in the same way as Table S6 in [2], considering the effect of weekends, holidays, school closures, and physical distancing and cocooning of high-risk populations based on the risk stage. Stages correspond to distancing stages of different strictness, which govern the reduced number of daily contacts people make relative to baseline. In our model, this is reflected by a coefficient $\kappa_i, i \in \mathcal{I}$, where $\kappa_i = 0.75$ would reduce the expected number of contacts to 25% of the baseline value. For the age group of 65 years and older and for the high-risk group, we use reductions based on cocooning, which are represented by coefficients $c_i, i \in \mathcal{I}$:

$$\phi_{i,t}^{a',r',a,r} = \begin{cases} (1-\kappa_i)\left[(1-1_{\{\text{off day}\}})\cdot(1-1_{\{\text{school closure}\}})\cdot\mathcal{S}_{a',a}+\right. & \text{if } a', a \in \{\text{0-4yr, 5-17yr, 18-49yr, 50-64yr}\}, \\ \quad \left.(1-1_{\{\text{off day}\}})\cdot\mathcal{W}_{a',a}+\mathcal{H}_{a',a}+\mathcal{O}_{a',a}\right] & \quad r', r \neq \text{high-risk} \\ (1-c_i)\left[(1-1_{\{\text{off day}\}})\cdot(1-1_{\{\text{school closure}\}})\cdot\mathcal{S}_{a',a}+\right. & \\ \quad \left.(1-1_{\{\text{off day}\}})\cdot\mathcal{W}_{a',a}+\mathcal{H}_{a',a}+\mathcal{O}_{a',a}\right] & \text{otherwise.} \end{cases} \quad [4]$$

The indicator $1_{\{\text{off day}\}}$ takes value 1 if the day is a weekend or holiday and is otherwise 0, and a similar indicator accounts for school closures. When a high-risk group, along with those 65 years and older, is involved either on the "giving" or "receiving" end of a contact, Eq. [4] assumes reduced transmission via the cocooning coefficient, c_i.

The following are key dates during the pandemic in Texas, and some define time blocks, which we use in estimating time-varying transmission reduction factors and other key model parameters as we describe shortly:

- February 28, 2020: Seed date for simulation of Austin, assuming seeding by a single symptomatic individual age 18-49y. This corresponds to 14 days prior to the first detected COVID-19 case in Austin on March 13, 2020.
- March 24, 2020: Austin's Stay Home-Work Safe Order is enacted at midnight [5].
- May 1, 2020: The Governor of Texas relaxed physical distancing orders statewide [6].
- May 21, 2020: Just prior to Memorial Day Weekend.
- June 26, 2020: The Governor of Texas issued an executive order limiting service at bars and restaurants, and Travis County (which includes Austin) banned gatherings of more than 100 people [7, 8].
- July 17, 2020: Time point in hospitalization data suggesting a change in dynamics.
- August 9, 2020: The last day of observed data from the hospital system used in estimating changes in ICU dynamics.
- August 20, 2020: First day students returned to residence halls at the University of Texas at Austin.
- October 7, 2020: The last day of observed data used in estimating model parameters.

We assume that there are six time blocks denoted by $\mathcal{T}_j$ for $j \in \{1, 2, 3, 4, 5, 6\}$ as defined in Table 2. They guide fitting of transmission-reduction parameters, κ and c, and certain dynamics in use of the ICU and hospital duration, as detailed below.

We model the hospitalization dynamics, including proportions of hospitalized requiring the ICU and durations in the general ward and ICU, using data from a multi-facility hospital system serving the central

Time Block	Start Date	End Date	Definition
$\mathcal{T}_1$	2/28/20	3/23/20	unmitigated transmission before first stay-home order
$\mathcal{T}_2$	3/24/20	5/20/20	effective period for first stay-home order
$\mathcal{T}_3$	5/21/20	6/25/20	relaxed period starting with Memorial Day weekend
$\mathcal{T}_4$	6/26/20	7/16/20	period of effective physical distancing
$\mathcal{T}_5$	7/17/20	8/19/20	period distinguished by changes in ICU dynamics
$\mathcal{T}_6$	8/20/20	10/7/20	period of effective physical distancing

Table 2: The five time blocks, $\mathcal{T}_1$, $\mathcal{T}_2$, $\mathcal{T}_3$, $\mathcal{T}_4 \cup \mathcal{T}_5$, and $\mathcal{T}_6$ correspond to different rates of spread, as estimated using transmission-reduction factors κ and c. The fourth and fifth time blocks, $\mathcal{T}_4$ and $\mathcal{T}_5$, differ only in dynamics involving the ICU, both the admission probability and the sojourn time in the general ward prior to ICU admission.

Texas region, including Austin, Texas ("hospital system data"). Conditional on being admitted to the hospital, we observe a decreasing trend in the probability a patient is admitted to the ICU throughout the time horizon, which holds for both direct admissions to the ICU and patients who are first admitted to the general ward. Among patients who enter the general ward and are then admitted to the ICU, their duration of stay in the general ward, determined by η_{ICU}, grows over time. For each time block, $\mathcal{T}_j$, we assume a constant $\eta_{ICU,j}$ and further assume a constant daily decrease, r_j, on both of the fractions, p_{IH} and $HICUR$:

$$p_{IH,t+1} = r_j p_{IH,t} \qquad \forall j \in \{1,2,3,4,5,6\}, t \in \mathcal{T}_j \qquad \text{[5a]}$$

$$HICUR_{t+1} = r_j HICUR_t \qquad \forall j \in \{1,2,3,4,5,6\}, t \in \mathcal{T}_j, \qquad \text{[5b]}$$

along with a similar decrement across boundaries of the blocks. We use duration times for each time block from the hospital system data to estimate $\eta^a_{ICU,j}$ and fit r_j, with the estimated parameters in Table 3.

	age group	$\mathcal{T}_1$	$\mathcal{T}_2$	$\mathcal{T}_3$	$\mathcal{T}_4$	$\mathcal{T}_5 \cup \mathcal{T}_6$
$\eta^a_{ICU,j}$	0-4 yr	0.5882	0.5882	0.3885	0.2640	0.2589
	5-17 yr	0.5882	0.5882	0.3885	0.2640	0.2589
	18-49 yr	0.5882	0.5882	0.3885	0.2640	0.2589
	50-64 yr	0.6273	0.6273	0.4143	0.2815	0.2761
	$\geq$ 65 yr	0.6478	0.6478	0.4278	0.2907	0.2851
r_j		0.9973	0.9973	0.9932	0.9921	1

Table 3: Estimates of ICU admission probability parameters, η_{ICU}, p_{IH}, and $HICUR$; see Fig. 1 and accompanying parameter definitions. For each age group, a, and each time block, j, we specify η_{ICU}, and we give the daily decrement factor, r_j, used in Eq. [5].

Using the hospital system data, and consistent with the transition diagram in Fig. 1, we define the ICU duration for a patient as the time between their admission to the ICU and their discharge from the hospital. The reality is more complex as ICU patients typically return to the general ward prior to discharge from the hospital, and iterations between the two units, driven by a patient's health status, can also occur. Therefore, the reported duration in the ICU leads to over estimating ICU utilization and under-estimating that of the general ward. To handle this in our model, we introduce two constant parameters, α_{ICU} and α_H, to better

estimate durations in the ICU and general ward and better represent their respective utilization:

$$\begin{aligned}\gamma_H &= (1-\alpha_H)\gamma_H^0\\ \gamma_{ICU} &= (1+\alpha_{ICU})\gamma_{ICU}^0\\ \mu &= (1+\alpha_{ICU})\mu^0,\end{aligned}$$

where γ_H^0, γ_{ICU}^0, and μ^0 are obtained from the hospital system data, with each row corresponding to an age group in ascending order:

$$\gamma_H^0 = \begin{bmatrix}0.2399\\0.2399\\0.2399\\0.2222\\0.2124\end{bmatrix},\ \gamma_{ICU}^0 = \begin{bmatrix}0.0700\\0.0700\\0.0700\\0.0575\\0.0518\end{bmatrix},\ \mu^0 = \begin{bmatrix}0.0749\\0.0749\\0.0749\\0.0766\\0.0799\end{bmatrix},$$

with units of day^{-1}.

The bulk of the epidemiological and hospitalization parameters are specified above or are detailed in Tables 7 and 8, with the latter obtained from the literature or information collected from local healthcare agencies. The time blocks are specified in Table 2. Given these, we estimate 14 parameters, but with 7 degrees of freedom, as we detail below. We perform the fit of the deterministic SEIR model in Eqs. [1] using: (i) daily COVID-19 admissions, denoted H_t and available for Austin only; (ii) a daily COVID census in the general ward, IH_t; and (iii) a daily COVID census in the ICU, ICU_t, all on day t. By minimizing a weighted sum of least-square errors, we estimate $\hat{\kappa}_j$ and $\hat{c}_j$, $j = 1, 2, \ldots, 6$, α_H, and α_{ICU}, using SciPy/Python [9] via `scipy.optimize.least_squares`. We use the "hat" notation on κ and c to distinguish, for example, $\hat{\kappa}_j$ for *time block* j (see Table 2) from κ_i, which corresponds to *stage* i per Eq. [4], and show the mapping shortly.

We minimize

$$\sum_t (IH_t - \widehat{IH}_t)^2 + w_{ICU}^2 \sum_t (ICU_t - \widehat{ICU}_t)^2 + w_H^2 \sum_t (H_t - \widehat{H}_t)^2,$$

where $\widehat{IH}_t$, $\widehat{ICU}_t$, and $\widehat{H}_t$ denote the estimated IH_t, ICU_t, and H_t obtained through Eqs. [1]; w_{ICU} and w_H are scaling constants; and the sum is over $t \in \mathcal{T}_1 \cup \cdots \cup \mathcal{T}_6$. We assume $w_{ICU} = 1.50$ and $w_H = 7.58$, as those values approximate magnitudes relative to that of the general ward. To obtain a parsimonious model, we use $\hat{c}_1 = 0$, $\hat{c}_2 = \hat{c}_3 = \hat{\kappa}_2$, $\hat{c}_4 = \hat{c}_5 = \hat{\kappa}_4 = \hat{\kappa}_5$ and $\hat{c}_6 = \hat{\kappa}_6$, which reduces the number of estimated parameters from 14 to 7. The rationale is that there was effectively no cocooning during the initial time block $\mathcal{T}_1$, and thus we set $\hat{c}_1 = 0$. Because physical distancing was stricter over time block $\mathcal{T}_2$ than time block $\mathcal{T}_3$, and the cocooning effectiveness parameters are expected to be at least that of the distancing parameters, we use $\hat{c}_2 = \hat{c}_3 = \hat{\kappa}_2$. Because of behavioral changes over time, including increased use of face-masks, when we perform the fit we observe greater reduction in transmission in time blocks 4 and 5 than we do in block 2, and so we use $\hat{c}_4 = \hat{\kappa}_4$. Finally, while hospitalization parameters differ over time blocks $\mathcal{T}_4$ and $\mathcal{T}_5$, rates of transmission do not appear to differ significantly, and so we consider $\hat{c}_4 = \hat{c}_5 = \hat{\kappa}_4 = \hat{\kappa}_5$.

We use the trust region reflective algorithm (`trf`) in `scipy.optimize.least_squares`, with lower and upper bounds on each parameter of 0 and 1, respectively. The algorithm obtains locally optimal values of the parameters, the quality of which has been validated by comparing projections with the observed

j	$\hat{\kappa}_j$	$\hat{c}_j$
1	0.0613	0.0000
2	0.7436	0.7436
3	0.6026	0.7436
4	0.7815	0.7815
5	0.7815	0.7815
6	0.7544	0.7544
α_H	0.2862	
α_{ICU}	0.5621	

Table 4: Fitted transmission reduction parameters, $\hat{\kappa}_j$, and cocooning effectiveness parameters, $\hat{c}_j$, for each time block $\mathcal{T}_j$, along with estimated hospitalization duration adjustment parameters, α_H and α_{ICU}.

data. All the remaining parameters are set to their default values (see above and Tables 7 and 8). The fitted values for $\hat{\kappa}_j$ and $\hat{c}_j$ and α_H and α_{ICU} are given in Table 4.

The physical distancing parameters for each stage are mapped to κ_i and c_i for $i \in \mathcal{I}$ based on the historical implementation of the policy. We set:

$$\kappa_1 = \hat{\kappa}_4 \qquad c_1 = \hat{\kappa}_4 \qquad \text{[6a]}$$

$$\kappa_2 = \frac{\hat{\kappa}_4 + \hat{\kappa}_3}{2} \qquad c_2 = \hat{\kappa}_2 \qquad \text{[6b]}$$

$$\kappa_3 = \hat{\kappa}_3 \qquad c_3 = \hat{\kappa}_2 \qquad \text{[6c]}$$

$$\kappa_4 = \hat{\kappa}_3 - \frac{\hat{\kappa}_4 - \hat{\kappa}_3}{2} \qquad c_4 = 1 - 1.25 \cdot (1 - c_2). \qquad \text{[6d]}$$

In Eq. [6a] we set κ_1 (red) to the strictest observed level of transmission reduction, June 26–August 19, 2020. In Eq. [6c] we set κ_3 (yellow) to the relaxed period of relatively high transmission, roughly from Memorial Day weekend through June 25, 2020. Eq. [6b] forms κ_2 (orange) as the average between these two levels of reduction. The most relaxed stage of transmission reduction we consider (blue), uses the same increment between the red and orange stages and between orange and yellow in Eq. [6d]. We do not separately estimate cocooning, but assume it matches the strictest level of reduction in the low-risk population when in the red stage, that observed during the stay-home period after March 24th for the orange and yellow stages, and then in the blue stage relaxes by a 25% increment, as shown in Eq. [6d], so that a reduction of 0.75 would drop to 0.6875. The $X_{i,t,\omega}$ parameters in Equations [1] allow us to compactly represent, in the mathematical model, the current stage of transmission over the history of the pandemic. In our analysis, we fix future transmission rate at a given point estimate for future time periods.

Selection of Scenarios

After fitting the parameters via least-squares minimization using the procedure just described, we simulate a set of scenarios, Ω. There are macro stochastics, involving modeling σ, ω_A, γ_A, and γ_Y as random variables; see Table 7. And, micro stochastics govern a binomially distributed number of transitions between compartments. Inevitably, some stochastic sample paths will yields hospitalizations that diverge from observed data, including sample paths in which spread quickly terminates after initializing with a single infectious person.

Here we describe how we select scenarios, sampled from the marginal distributions of σ, ω_A, γ_A, and γ_Y, and from the micro-stochastics process, in order to generate a set of 300 scenarios, indexed by $\omega \in \Omega$

Algorithm 1: Pseudo-code for the sampling procedure

1 Initialize $\Omega = \emptyset$
2 **while** $|\Omega| < 300$ **do**
3 **for** $j = 1, \ldots, 6$ **do**
4 **if** $j == 1$ **then**
5 Generate a scenario (sample path) ω over time block $\mathcal{T}_1$
6 **else**
7 Continue simulating scenario ω over time block $\mathcal{T}_j$
8 Compute $R^2 = 1 - \frac{\sum_{t \in \mathcal{T}_1 \cup \cdots \cup \mathcal{T}_j} (IH_t - \widehat{IH}_t)^2}{\sum_{t \in \mathcal{T}_1 \cup \cdots \cup \mathcal{T}_j} (IH_t - \overline{IH})^2}$
9 **if** $R^2 < 0.85$ **then**
10 break and initiate next ω and $j = 1$
11 $\Omega \leftarrow \Omega \cup \{\omega\}$

and used in Eqs. [1]. Because the projections at earlier time points guide the trigger optimization model at later time points, the goal is to start the latter with scenarios, $\omega \in \Omega$, that are consistent with observed hospitalizations up to that point in time. In order to evaluate the quality of scenario ω in this sense, we use

$$R^2 = 1 - \frac{\sum_t (IH_t - \widehat{IH}_t)^2}{\sum_t (IH_t - \overline{IH})^2},$$

where $\overline{IH}$ is the mean of the IH_t values. Algorithm 1 summarizes the sampling procedure to generate $|\Omega| = 300$ scenarios.

Algorithm 1 uses the six time blocks $\mathcal{T}_j$, $j = 1, 2, 3, 4, 5, 6$, given in Table 2. We start with simulating a sample path ω during the first time block $\mathcal{T}_1$ (see line 4–5), and compute the corresponding R^2 value at the end of $\mathcal{T}_1$. If the scenario, ω, has the desired quality over $\mathcal{T}_1$, i.e., $R^2 \geq 0.85$, we continue simulating the path ω. At the end of each time block, we compute the corresponding R^2 value as shown in line 8, and decide whether the path is kept or discarded, as shown in lines 9–10. Here, the threshold value 0.85 of R^2 is a tuning parameter, which we return to below. Once Algorithm 1 provides 300 scenarios at the end of time block $\mathcal{T}_6$, we continue simulating them for use in the stochastic optimization model [3] over the rest of the time horizon.

Fig. 2 show histograms of the resulting marginal distributions from Algorithm 1 for σ, ω_A, γ_A, and γ_Y. The scatter plots of Fig. 3 again use the scenarios, Ω, obtained by Algorithm 1 to give insight to bivariate dependencies. We generate random variables from the independent nominal triangular distributions given in Table 7, and Algorithm 1 "accepts" those that are consistent with observed hospitalizations. The resulting marginal distributions can differ from the nominal distribution; see the distribution of ω_A in Fig. 2. In addition, even though we sample independently from the nominal distributions, Algorithm 1 can induce dependence; see the strong negative correlation between ω_A and $1/\gamma_Y$ in Fig. 3.

For the purpose of visualizing results we use spaghetti plots that detail 300 sample paths, and we also use a single "representative" path. A simple least-squares selection of a path from the collection of 300 paths

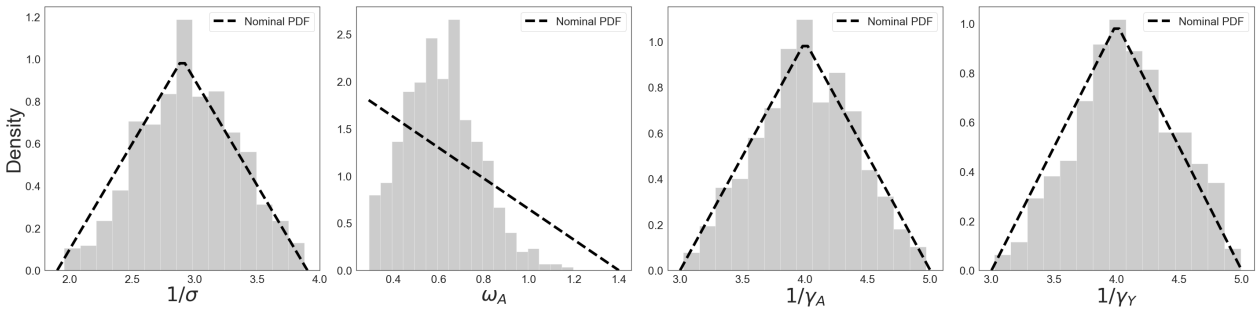

Figure 2: Histogram of the random variables σ, ω_A, γ_A, and γ_Y for the scenario set Ω obtained by Algorithm 1. Rather than showing the rates, we show $1/\sigma$, $1/\gamma_A$, and $1/\gamma_Y$, which correspond to durations in days. We sample from the marginal distributions of each of the four parameters, and Algorithm 1 accepts sample paths consistent with hospitalizations, while also sampling a binomial number of transitions between compartments in the SEIR-style model. While there are modest deviations from the nominal triangular distributions for durations ($1/\sigma$, $1/\gamma_A$, and $1/\gamma_Y$), the distribution of the relative infectiousness of an asymptomatic individual (ω_A) deviates significantly from its nominal distribution.

arguably does *not* yield a representative path. Because the timing of peaks in paths differs, the simple least-squares path is "flatter" through the cloud than most paths. Here we describe how we select a representative path from the collection of 300.

We define a selection criterion based on metrics of interest, such as the total number of people hospitalized in the general ward over the duration, the peak number of people in the hospital, and the time of that peak. We let $\widehat{IH}_{t,\omega}$, $\widehat{ICU}_{t,\omega}$, and $\widehat{H}_{t,\omega}$ denote the estimates of IH_t, ICU_t, and H_t for each sample path, $\omega \in \Omega$, and we first obtain the squared deviations from the observed data, defining $Z_{\omega,obs}$ as follows:

$$Z_{\omega,obs} = \sum_t (\widehat{IH}_{t,\omega} - IH_t)^2 + w_{ICU}^2 \sum_t (\widehat{ICU}_{t,\omega} - ICU_t)^2 + w_H^2 \sum_t (\widehat{H}_{t,\omega} - H_t)^2,$$

where w_{IH} and w_{ICU} are scaling constants. Here, t ranges over all days up to October 7, 2020, for which we have observed data. We then define metrics to represent the statistical properties of the scenarios as in Table 5.

Metric	Definition	Standardized Metric
$IH_{\omega,tot} = \sum_{t=1}^{T} IH_{t,\omega}$	Total number of patient-days	$Z_{\omega,IH_{tot}} = (IH_{\omega,tot} - \hat{\mu}_{IH_{tot}})/\hat{\sigma}_{IH_{tot}}$
$IH_{\omega,max} = \max_t IH_{t,\omega}$	Peak hospitalization	$Z_{\omega,IH_{max}} = (IH_{\omega,max} - \hat{\mu}_{IH_{max}})/\hat{\sigma}_{IH_{max}}$
$IH_{\omega,med} = \text{median}_t IH_{t,\omega}$	Median hospitalization	$Z_{\omega,IH_{med}} = (IH_{\omega,med} - \hat{\mu}_{IH_{med}})/\hat{\sigma}_{IH_{med}}$
$t_{\omega,IH_{max}} = \arg\max_t IH_{t,\omega}$	Timing of hospitalization peak	$Z_{t_{\omega,IH_{max}}} = (t_{\omega,IH_{max}} - \hat{\mu}_{t_{IH_{max}}})/\hat{\sigma}_{t_{IH_{max}}}$

Table 5: Metrics for hospitalized patients in the general ward under each sample path ω. Note that $\hat{\mu}$ and $\hat{\sigma}$ represent the sample mean and sample standard deviation for each metric, across the $|\Omega| = 300$ sample paths.

Analogs of the standardized metrics for those hospitalized in the general ward (IH) from Table 5 are also computed for those hospitalized in the ICU (ICU), and new daily hospital admissions (H) to form a total of 12 such metrics. We select the representative scenario ω' such that

$$\omega' \in \arg\min_{\omega \in \Omega} \left(\frac{w_{std}}{12} Z_{\omega,std} + w_{obs} Z_{\omega,obs} \right) \quad [7]$$

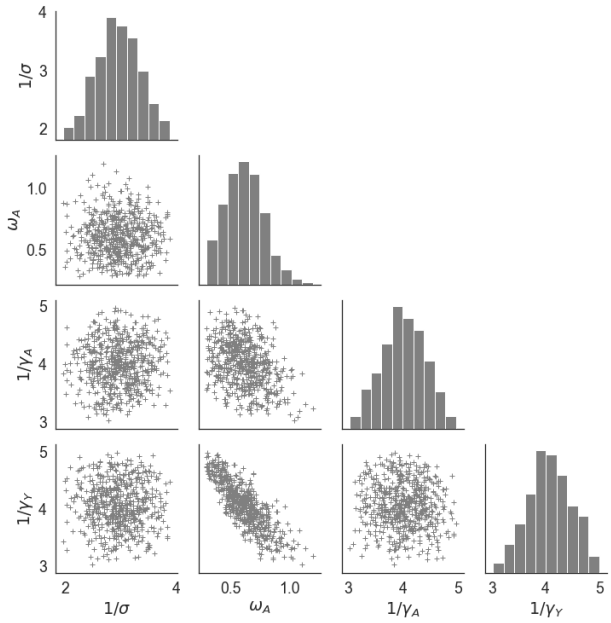

Figure 3: Scatter plot of the random variables $1/\sigma$, ω_A, $1/\gamma_A$, and $1/\gamma_Y$ for the scenario set Ω selected by Algorithm 1. We sample *independently* from the marginal distributions of each of the four parameters, and the algorithm accepts sample paths consistent with hospitalizations. This can induce dependencies as shown, for example, between $1/\gamma_Y$ and ω_A.

where

$$\begin{aligned} Z_{\omega,std} = & Z^2_{\omega,IH_{tot}} + Z^2_{\omega,IH_{max}} + Z^2_{\omega,IH_{med}} + Z^2_{\omega,t_{IH_{max}}} \\ & + Z^2_{\omega,ICU_{tot}} + Z^2_{\omega,ICU_{max}} + Z^2_{\omega,ICU_{med}} + Z^2_{\omega,t_{ICU_{max}}} \\ & + Z^2_{\omega,H_{tot}} + Z^2_{\omega,H_{max}} + Z^2_{\omega,H_{med}} + Z^2_{\omega,t_{H_{max}}}, \end{aligned}$$

where w_{std} and w_{obs} are positive weights that sum to one. This method is used to select the representative paths plotted in the main text.

ACS Parameters

Table 6 details parameters used to analyze ACS triggers, involving weighted combinations of transmission reduction between the orange and yellow stages. The stages differ in the physical distancing coefficient, κ, but all use the same cocooning coefficient, c, as shown in the table.

We assume the ACS can be set up within two weeks; i.e., the ACS will be ready to use 14 days after the trigger threshold is reached. In reality, an ACS is built in phases with staffing being the final phase that allows the facility to function. The trigger threshold to operationalize and size the ACS are both selected by a grid search with the grid step sizes of 10 and 50, respectively, although the latter can be selected in a pre-processing step, prior to the optimization, as described above.

Transmission Reduction		κ	c
orange	yellow		
100%	0%	0.7164	0.7437
50%	50%	0.6837	0.7437
0%	100%	0.6510	0.7437

Table 6: The two left-most columns indicate the relative weight on transmission reduction factors for the orange and yellow stages. So, the last row corresponds to yellow, while the 50-50% row corresponds to equal weight on the orange and yellow values. The two right-most columns show the resulting transmission reduction coefficients for the low-risk population (κ) and the high-risk population (c) for Austin.

Parameters	Values	Source
β: transmission rate	0.06901	[2, 10]
P: proportion of pre-symptomatic transmission (%)	44	[3]
ω_A: infectiousness of individuals in compartment IA, relative to IY	$\omega_A \sim$ Triangular (0.29,0.29,1.4)	[11]
τ : symptomatic proportion (%)	57	[12]
ω_P: infectiousness of individuals in pre-symptomatic and pre-asymptomatic compartments, relative to symptomatic and asymptomatic compartments	$\omega_P = \frac{P}{1-P}\frac{\tau(\frac{YHR}{\eta_H}+\frac{1-YHR}{\gamma_Y})+(1-\tau)\frac{\omega_A}{\gamma_A}}{\frac{\tau}{\rho_Y}+(1-\tau)\frac{\omega_A}{\rho_A}}$	
σ : exposed rate	$\frac{1}{\sigma} \sim$ Triangular (1.9, 2.9, 3.9)	Based on incubation [13] and pre-symptomatic periods
γ_A: recovery rate from compartment IA	$\frac{1}{\gamma_A} \sim$ Triangular (3, 4, 5)	[3]
γ_Y: recovery rate from symptomatic compartment IY	$\frac{1}{\gamma_Y} \sim$ Triangular (3, 4, 5)	[3]
ρ_A: rate at which pre-asymptomatic individuals become asymptomatic	Equal to ρ_Y	[3]
ρ_Y: rate at which pre-symptomatic individuals become symptomatic	$\frac{1}{\rho_Y} = 2.3$	[3]
IFR: infected fatality ratio, age specific (%)	Low risk / High risk 0.000917 / 0.00917 0.00218 / 0.0218 0.0339 / 0.339 0.252 / 2.52 0.644 / 6.44	Age adjusted from [14]
YFR: symptomatic fatality ratio, age specific (%)	Low risk / High risk 0.00161 / 0.0161 0.00382 / 0.0382 0.0594 / 0.594 0.442 / 4.42 1.13 / 11.3	$YFR = \frac{IFR}{1-\tau}$
C: daily cost to stay at specific stages	C_1 10000 C_2 100 C_3 10 C_4 1	

Table 7: Model parameters

Parameters	Value	Source
η_H : rate from symptom onset to hospital admission	0.1695	5.9 day average from symptom onset to hospital admission [15]
YHR: symptomatic case hospitalization rate (%)	Low risk / High risk 0.0279 / 0.2791 0.0215 / 0.2146 1.3215 / 13.2514 2.8563 / 28.5634 3.3873 / 33.8730	Age adjusted from [14]
p_{IH}	Fitted time series, starting at 0.6717	hospital system data
γ_H, γ_{ICU} : recovery rate in compartment IH and ICU	Fitted parameters	hospital system data
π : rate symptomatic individuals go to hospital, age-specific	$\pi = \frac{\gamma_Y \cdot YHR}{\eta_H + (\gamma_Y - \eta_H)YHR}$	
η_{ICU} : rate from hospital admission to ICU	A time series which is constant specific to time blocks	hospital system data
μ : rate from ICU to death	Fitted parameters	hospital system data
$ICUFR$: ICU death ratio, age specific (%)	$ICUFR$ 5.8592 5.8592 5.8592 15.6207 30.8526	hospital system data
$HICUR$: hospitalized ICU ratio	A time series with a decreasing rate specific to time blocks, starting at 0.1574	hospital system data
ν_H : ICU rate on hospitalized individuals, age-specific	$\nu_H = \frac{\gamma_H * HICUR}{\eta_{ICU} + (\gamma_H - \eta_{ICU})HICUR}$	
ν_{ICU} : death rate on ICU individuals, age-specifc	$\nu_{ICU} = \frac{\gamma_{ICU} * ICUFR}{\mu + (\gamma_{ICU} - \mu)ICUFR}$	
B: Total hospital bed capacity (including ICU)	1500	Estimates provided by Austin area hospital systems and aggregated by public health leaders
$1_{\{\text{school closure}\}}$: school closure dates	$3/19/2020 - 9/8/2020$, $5/26/2021 - 8/23/2021$	

Table 8: Hospitalization parameters

Acknowledgements

The use of the hospital system data to generate the input model parameters was approved as exempt human subjects research by the IRB of The University of Texas at Austin.

References

[1] Wang, X. *et al.* Impact of social distancing measures on coronavirus disease healthcare demand, central texas, USA. *Emerging Infectious Diseases* **26**, 2361–2369 (2020).

[2] Duque, D. *et al.* Timing social distancing to avert unmanageable COVID-19 hospital surges. *Proceedings of the National Academy of Sciences* (2020).

[3] He, X. *et al.* Temporal dynamics in viral shedding and transmissibility of COVID-19. *Nature Medicine* **26**, 672–675 (2020).

[4] Centers for Disease Control and Prevention. 500 cities: Local data for better health (2019). URL https://www.cdc.gov/500cities/definitions/health-outcomes.htm.

[5] The Mayor of the City of Austin. STAY HOME – WORK SAFE ORDER NO. 20200413-009, The City of Austin (2020). URL http://www.austintexas.gov/sites/default/files/files/document_96DEBEEC-E581-05E0-8A3D444404948A84.pdf.

[6] The Governor of Texas. Executive Order GA18: Relating to the expanded reopening of services as part of the safe, strategic plan to open Texas in response to the COVID-19 disaster (2020). URL https://gov.texas.gov/uploads/files/press/EO-GA-18_expanded_reopening_of_services_COVID-19.pdf.

[7] The Governor of Texas. Executive Order GA28: Relating to the targeted response to the COVID-19 disaster as part of the reopening of Texas (2020). URL https://gov.texas.gov/uploads/files/press/EO-GA-28_targeted_response_to_reopening_COVID-19.pdf.

[8] The Mayor of the City of Austin. Order 20200626-016: Stay home, mask, and otherwise be safe (2020). URL https://www.austintexas.gov/sites/default/files/files/Health/Order%20No.%2020200626-016-StayHome-Mask-Otherwise-Be-Safe.pdf.

[9] Virtanen, P. *et al.* SciPy 1.0: Fundamental Algorithms for Scientific Computing in Python. *Nature Methods* (2020).

[10] Yang, H. *et al.* Staged strategy to avoid hospital surge and preventable mortality, while reducing the economic burden of social distancing measures. Tech. Rep., The University of Texas at Austin (2020).

[11] He, D. *et al.* The relative transmissibility of asymptomatic cases among close contacts. *International Journal of Infectious Diseases* **94**, 145–147 (2020).

[12] Gudbjartsson, D. F. *et al.* Spread of SARS-CoV-2 in the Icelandic population. *New England Journal of Medicine* **382**, 2302–2315 (2020).

[13] Lauer, S. A. *et al.* The incubation period of coronavirus disease 2019 (COVID-19) from publicly reported confirmed cases: Estimation and application. *Annals of Internal Medicine* (2020).

[14] Verity, R. *et al.* Estimates of the severity of coronavirus disease 2019: a model-based analysis. *The Lancet Infectious Diseases* **20**, 669–677 (2020).

[15] Tindale, L. *et al.* Transmission interval estimates suggest pre-symptomatic spread of COVID-19. *Preprint* (2020).